# Adaptive observer design for uncertain hyperbolic PDEs coupled with uncertain LTV ODEs; Application to refrigeration systems

Mohammad Ghousein, Emmanuel Witrant

# Adaptive observer design for uncertain hyperbolic PDEs coupled with uncertain LTV ODEs; Application to refrigeration systems

Mohammad Ghousein [a], Emmanuel Witrant [b],

[a] *Université de Poitiers, LIAS laboratory, 2 rue Pierre Brousse, 86073 Poitiers, France*

[b] *Université Grenoble Alpes (UGA), GIPSA-lab, 11 rue des mathématiques, 38400 Saint-Martin-d'Hères, France*

**Abstract**

The problem of estimating the temperatures and the heat transfer coefficient of a concentric tube heat exchanger coupled with a heater is considered in this work. Measurements collected from the extremities of the exchanger tube are used to estimate the heat distribution over the length of the exchanger, which induces a boundary estimation problem. This system, which is part of any standard cooling plant, is particularly challenging due to the distributed nature of its variables. It is modeled by a system of $(2 \times 2)$ hyperbolic PDEs, coupled with an ODE at the boundary. To solve the estimation problem, we consider a general class of systems consisting of a $(2 \times 2)$ hyperbolic system coupled with a set of $n_X$ linear time-varying (LTV) ODEs at the boundary. Both the PDE and the ODEs have uncertain parameters to be estimated. The objective is to estimate the PDE states, the ODE states, and the parameters simultaneously with no assumption on the ODEs stability. We design a Luenberger state observer, and our method is mainly based on the decoupling of the PDE estimation error states from that of the ODEs via swapping design. We then derive the observer gains from the Lyapunov analysis of the decoupled system after proving the boundedness of the swapping filters. We give sufficient conditions of the exponential convergence of the adaptive observer through differential Lyapunov inequalities (DLIs). Finally, we apply the developed theory on the coupled heat exhanger-heater model to evaluate the performance of the observer in numerical simulations.

*Key words:* Adaptive boundary observers, Parameter estimation, Hyperbolic partial differential equations, Linear time-varying systems, Refrigeration systems.

## 1 Introduction

Refrigeration systems or human-made cooling systems are used to cool a substance or a closed space by transferring heat from a cold reservoir to a hot reservoir by means of an external mechanical intervention. These systems are found in many applications: food production, gas and oil industries, air conditioning of houses, buildings, big centers, cars and many more [12]. A refrigeration system is usually composed of the following main components: pumps, heat exchangers, heaters, expansion valves, chillers and accumulators. These parts are connected together to form what is called a refrigeration cycle. In this paper, we consider the refrigeration cycle shown on Figure 1. The objective of this cycle is to cool some electrical equipment that generates a heating power $U(t)$ while functioning. A real test bench for this system is already built at CERN [24] to cool the silicon sensors of high energy physics experiments. It works as follows: the cold fluid is pumped into the heat exchanger inner tube. Flowing inside the exchanger, the cold fluid gains energy from the hot fluid flowing in the opposite direction. Inside the heater, the cold fluid absorbs the heat from the electrical equipment and leaves the heater with high temperature. The hot fluid then recirculates back in the outer tube of the heat exchanger. At the output of the exchanger, the hot fluid is cooled down by the chiller and it is sent back to the pump to complete one cycle of cooling. The role of the accumulator is to maintain a desired output pressure at the hot side.

One component of this cycle that requires a special attention in modeling and in control is the heat exchanger. The temperatures and the other thermodynamical variables do not vary only with time but also along the

*Email addresses:* mohammad.ghousein@univ-poitiers.fr (Mohammad Ghousein), emmanuel.witrant@gipsa-lab.grenoble-inp.fr (Emmanuel Witrant).

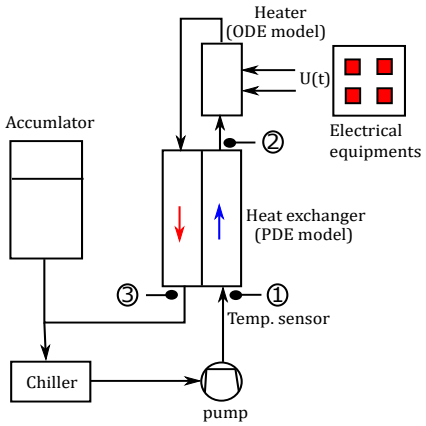


Fig. 1. Schematic diagram of a cooling cycle

length. The heat exchanger thus has distributed parameters and can spread along large distances and lead to significant delays in the refrigeration loop. In order to have low rates of energy consumption while maximizing the heat transfer rates, the control and the estimation algorithms must handle the distributed nature of the physical variables. Inside the heat exchanger, the hot fluid and the cold fluid exchange energy through the wall interface (see Figure 1). The parameter that controls this transfer of energy is called the heat transfer coefficient (HTC) and is usually difficult to estimate as it depends on many thermodynamical variables. In our recent work [15], we have solved the problem of estimating the distributed temperatures and the HTC of a concentric-tube heat exchanger using only four temperature measurements (provided by sensors placed at the extremities of the exchanger). The heat exchanger was separated from the other parts of the refrigeration network by assuming that all the input/output temperatures of the heat exchanger are measured. The cost of this strategy of modeling is to place four temperature sensors, at the inlets and at the outlets of the heat exchanger.

In this paper, we consider the coupled heat exchanger - heater model shown on Figure 1. The advantage of introducing the heater in the model, compared to previous designs such as [31,15], is to dispense one (costly) sensor at the hot inlet of the exchanger. However, introducing the heater complicates the adaptive observer design because the resulting model becomes a coupled PDE/ODE system. In this case, the PDE system models the heat exchanger and the ODE system models the heater as we show on Figure 1. Before presenting our observer design, we give a summary of the related works on boundary estimation for coupled hyperbolic PDE/ODE systems.

The problem of estimating the states of hyperbolic PDEs coupled with ODEs is relatively new. A Luenberger observer for systems of linear and quasi-linear hyperbolic systems coupled with linear time-invariant (LTI) ODEs at the boundary is proposed by [8]. The hyperbolic PDEs are homogeneous i.e. the propagation is only in one direction and the LTI ODEs are assumed asymptotically stable. This approach was later extended by [13] to linear hyperbolic systems coupled with possibly unstable LTI systems. The idea is to keep the same observer architecture as in [8] and to use a non-diagonal quadratic Lyapunov function instead of a diagonal one. Sufficient conditions for the exponential stability of the observer are obtained, involving bilinear matrix inequalities. These methods, relying on the stability property derived by [27], [5], use dissipative boundary conditions to stabilize the estimation error. One drawback of using this kind of boundary conditions is that it imposes some restrictions on the magnitude of the coupling between the system states. This limitation can be overcome using the so-called backstepping-method. An invertible Volterra transformation then maps the original system into a target system with the desired stability properties, for which static boundary control and observer gains are synthesized to ensure the system convergence to a desired set in finite time. An observer for LTI systems with arbitrary constant delay in the sensor measurement, where the delay is interpreted as a first order transport equation and a backstepping observer is designed on the resulting coupled LTI-PDE system, is synthesized by [20]. This approach was later extended to hyperbolic systems coupled with an LTI system at the boundary [17], including heterodirectional transport [10] and a robust feedback perspective [11]. The mentioned results so far do not consider having unknown (or largely varying) parameters in the system, as it is the case for most practical applications. The refrigeration cycle considered here is an example of such applications, as an important coefficient, the HTC, is not known. This motivates the need for adaptive estimators.

The role of the adaptive estimator is to generate simultaneous estimates of the states and of the parameters.

While some results on adaptive observers for infinite dimensional systems can be traced back to the 1990s [9,4], the research interest for adaptive observers for hyperbolic PDEs is mostly more recent. Combined parameter estimation and observer design for a generic class of transport PDEs is considered by [26], where a computationally-efficient method for hyperbolic systems using the time-delay equivalency is also proposed. Adaptive design for hyperbolic PDEs is more formally considered in [25], to analyze and control crowd dynamics using a Lyapunov method. Backstepping methods have been considered by [6], in an output-feedback stabilization perspective, and by [21] for a system of hyperbolic PDEs representing a process of oil well drilling. A swapping design was introduced in this framework by [3] and a global perspective is provided by [2]. Linearizing the dynamics as a set of hetero-directional hyperbolic PDE, adaptive methods for traffic congestion control are proposed by [29].

Fewer results can be found on adaptive design for sys-

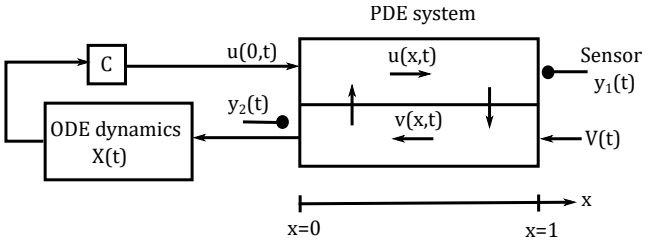


Fig. 2. Schematic diagram of the plant

tems of ODEs coupled with hyperbolic PDEs. Adaptation to fluctuations in the transport parameter for hyperbolic - ODE systems without in-domain couplings of the PDEs and with constant (in space) parameters can be addressed using the time-delay approach proposed by [30]. A (2×2) hyperbolic system coupled with an uncertain LTI system is considered by [1] and an adaptive observer is designed for the LTI part. An adaptive observer for a set of hyperbolic PDEs coupled with linear time varying (LTV) ODEs is considered by [14]: unknown parameters are only present on the ODEs side and the PDEs have a single direction of propagation.

Our contribution in this paper is to propose an adaptive estimator for a (2×2) hyperbolic system coupled with LTV ODEs at the boundary. The novelty of our design is to consider unknown parameters in the PDEs domain as well as in the ODE dynamics. In addition, the hyperbolic PDEs are hetero-directional: the two PDE states are propagating in opposite directions with a distributed coupling between them. All the states and parameters are estimated simultaneously in one step and without assumption on the asymptotic stability of the LTV ODEs. The proposed adaptive observer is evaluated on the estimation of the temperatures and the HTC of a coupled heat exchanger-heater system.

The paper is organized as follows. We formulate the estimation problem in Section 2. The adaptive observer design is detailed in Section 3. In Section 4 we present numerical simulations of the observer on an unstable toy plant. Section 5 is dedicated to the observer evaluation on the refrigeration cycle of Figure 1, and the paper is concluded in Section 6.

**Notations.** The symbol $S_+^n$ denotes the set of real $n \times n$ symmetric positive definite matrices. For a symmetric matrix $A$, positive and negative definiteness are denoted, respectively, by $A \succ 0$ and $A \prec 0$. For a vector $z \in \mathbb{R}^n$, $\left|z\right|$ is the euclidean norm. Let $V \subseteq \mathbb{R}^n$ and $f : [0,1] \longmapsto V$, we denote by $||f||_{\mathbb{L}^2([0,1])^n} = \sqrt{\int_0^1 \left|f(x)\right|^2 dx}$ the $L^2$ norm of $f$. If $f \in \mathbb{L}^2([0,1])^n$, then $||f||_{\mathbb{L}^2([0,1])^n} < +\infty$. $\partial_t$ and $\partial_x$ denote the partial derivatives with respect to space and time, respectively.

## 2 Problem statement

Consider the following $(2 \times 2)$ hyperbolic system evolving in $\{(t,x) \mid t \geq 0, x \in [0,1]\}$ and coupled with $n_X$ ordinary differential equations at the boundary $x = 0$:

$$\partial_t u(x,t) + \lambda_1(x)\partial_x u(x,t) = \sigma_1(x)v(x,t) + \phi_1(x,t)\theta_1 \quad (1)$$

$$\partial_t v(x,t) - \lambda_2(x)\partial_x v(x,t) = \sigma_2(x)u(x,t) + \phi_2(x,t)\theta_2 \quad (2)$$

$$u(0,t) = CX(t) \quad (3)$$

$$v(1,t) = V(t) \quad (4)$$

$$\dot{X}(t) = A(t)X(t) + B(t)U(t) + D(t)v(0,t) + \psi(t)\theta_3 \quad (5)$$

where $u(x,t)$ and $v(x,t)$ are the states, $[u,v]^T : [0,1] \times [0,+\infty) \to \mathbb{R}^2$. $\lambda_1(x) > 0$ and $\lambda_2(x) > 0$ are the PDEs transport velocities, considered as $C^1([0,1];\mathbb{R})$ known functions. $\sigma_1(x)$ and $\sigma_2(x)$, some $C^0([0,1];\mathbb{R})$ known functions, are the PDEs in-domain coupling terms. $\phi_1(x,t) : [0,1] \times [0,+\infty) \to \mathbb{R}^{1\times n_{\theta_1}}$ is a set of known bounded filters for the unknown parameters $\theta_1 \in \mathbb{R}^{n_{\theta_1}}$. Similarly, $\phi_2(x,t) : [0,1] \times [0,+\infty) \to \mathbb{R}^{1\times n_{\theta_2}}$ is a set of known bounded filters for the unknown parameters $\theta_2 \in \mathbb{R}^{n_{\theta_2}}$. $V(t)$ is a known boundary input acting on the right boundary of (2). $X(t) : [0,+\infty) \to \mathbb{R}^{n_X}$ is the ODE vector of states. $\theta_3 \in \mathbb{R}^{n_{\theta_3}}$ are the ODE unknown parameters. The PDE (1) is coupled with the ODE (5) at the left boundary through the output matrix $C \in \mathbb{R}^{1\times n_X}$. $U(t) : [0,+\infty) \to \mathbb{R}^{n_u}$ is the known ODE input vector. The ODE matrices $A(t) \in \mathbb{R}^{n_X \times n_X}$, $B(t) \in \mathbb{R}^{n_X \times n_u}$, $D(t) \in \mathbb{R}^{n_X \times 1}$ and $\psi(t) \in \mathbb{R}^{n_X \times n_{\theta_3}}$ are are assumed to be known, bounded and piece-wise continuous in time.

The goal is to estimate the distributed states of the PDEs $u(x,t)$ and $v(x,t)$, the ODE state $X(t)$ and the parameters $\theta_1$, $\theta_2$ and $\theta_3$ using the boundary measurements: $y_1(t) = u(1,t)$ and $y_2(t) = v(0,t)$. The schematic diagram of the plant (1)-(5) is shown on Figure 2. Some obvious conditions are necessary for the feasibility of this estimation problem. For example, if the output matrix $C$ is equal to zero, no information about the ODE dynamics $X(t)$ is measured by the sensor at $x = 1$ and hence the estimation of the ODE state will not be possible. Analogous conditions can be deduced for $\phi_1(x,t)$, $\phi_2(x,t)$ and $\psi(t)$. We will discuss the feasibility conditions for the estimation problem in the next sections. It is also helpful to discuss the reasons that can cause the plant (1)-(5) to be unstable in open loop, i.e. when $V(t) = 0$ and $U(t) = 0$. One reason is the PDE couplings $\sigma_1(x)$ and $\sigma_2(x)$. If these couplings are large enough, the plant (1)-(5) is unstable in open loop. The second reason is the stability of the ODE dynamics: if $A(t)$ is not stable then the whole plant (1)-(5) is unstable in open loop. These reasons are the key points in stabilizing the observation error dynamics. Note that we do not assume

that the plant is stable, i.e. we assume no conditions on the magnitude of $\sigma_1(x)$ and $\sigma_2(x)$ neither on the eigenvalues of $A(t)$. The observer architecture must take into account all these stability issues.

## 3 Adaptive observer design

We define the dynamics of the adaptive observer as follows:

$$\begin{aligned}&\partial_t\hat{u}(x,t)+\lambda_1(x)\partial_x\hat{u}(x,t)=\sigma_1(x)\hat{v}(x,t)+m_1(x,t)\\&+\phi_1(x,t)\hat{\theta}_1(t)-p_{y_1}(x,t)\big(\hat{u}(1,t)-y_1(t)\big)\\&-p_{y_2}(x,t)\big(\hat{v}(0,t)-y_2(t)\big)\end{aligned}\tag{6}$$

$$\begin{aligned}&\partial_t\hat{v}(x,t)-\lambda_2(x)\partial_x\hat{v}(x,t)=\sigma_2(x)\hat{u}(x,t)+m_2(x,t)\\&+\phi_2(x,t)\hat{\theta}_2(t)-r_{y_1}(x,t)\big(\hat{u}(1,t)-y_1(t)\big)\\&-r_{y_2}(x,t)\big(\hat{v}(0,t)-y_2(t)\big)\end{aligned}\tag{7}$$

$$\hat{u}(0,t)=q\big(\hat{v}(0,t)-y_2(t)\big)+C\hat{X}(t)\tag{8}$$

$$\hat{v}(1,t)=V(t)\tag{9}$$

$$\begin{aligned}&\dot{\hat{X}}(t)=A(t)\hat{X}(t)+B(t)U(t)+\psi(t)\hat{\theta}_3(t)\\&+D(t)\hat{v}(0,t)-L(t)(\hat{u}(1,t)-y_1(t))\end{aligned}\tag{10}$$

The estimates of the states are denoted by hat. $p_{y_1}(x,t)$, $p_{y_2}(x,t)$, $r_{y_1}(x,t)$ and $r_{y_2}(x,t)$ are the PDE observer gains, varying in space and time. $L(t)\in\mathbb{R}^{n_X\times 1}$ is the ODE observer gain, time-varying since the ODE dynamics are LTV. $m_1(x,t)$ and $m_2(x,t)$ are two feedback functions related to the parameters (to be defined later). $q\neq 0$ is a known parameter that can be chosen arbitrarily. The observer architecture (6)-(10) is of Luenberger type. The measurements $y_1(t)$ and $y_2(t)$ are injected in the PDE domain and in the ODE dynamics to correct the observer dynamics using linear gains. We define now the observation errors: $\tilde{u}(x,t)=u(x,t)-\hat{u}(x,t)$, $\tilde{v}(x,t)=v(x,t)-\hat{v}(x,t)$, $\tilde{X}(t)=X(t)-\hat{X}(t)$, $\tilde{\theta}_1(t)=\theta_1-\hat{\theta}_1(t)$, $\tilde{\theta}_2(t)=\theta_2-\hat{\theta}_2(t)$ and $\tilde{\theta}_3(t)=\theta_3-\hat{\theta}_3(t)$. The error dynamics can then be calculated from subtracting the observer equations (6)-(10) from the plant equations (1)-(5) to have:

$$\begin{aligned}&\partial_t\tilde{u}(x,t)+\lambda_1(x)\partial_x\tilde{u}(x,t)=\sigma_1(x)\tilde{v}(x,t)-m_1(x,t)\\&+\phi_1(x,t)\tilde{\theta}_1(t)-p_{y_1}(x,t)\tilde{u}(1,t)-p_{y_2}(x,t)\tilde{v}(0,t)\end{aligned}\tag{11}$$

$$\begin{aligned}&\partial_t\tilde{v}(x,t)-\lambda_2(x)\partial_x\tilde{v}(x,t)=\sigma_2(x)\tilde{u}(x,t)-m_2(x,t)\\&+\phi_2(x,t)\tilde{\theta}_2(t)-r_{y_1}(x,t)\tilde{u}(1,t)-r_{y_2}(x,t)\tilde{v}(0,t)\end{aligned}\tag{12}$$

$$\tilde{u}(0,t)=q\tilde{v}(0,t)+C\tilde{X}(t)\tag{13}$$

$$\tilde{v}(1,t)=0\tag{14}$$

$$\dot{\tilde{X}}(t)=A(t)\tilde{X}(t)+\psi(t)\tilde{\theta}_3(t)+D(t)\tilde{v}(0,t)-L(t)\tilde{u}(1,t)\tag{15}$$

The goal is to find the proper observer gains $p_{y_1}(x,t)$, $p_{y_2}(x,t)$, $r_{y_1}(x,t)$, $r_{y_2}(x,t)$ and $L(t)$, the adequate adaptive laws of the parameters $\hat{\theta}_1(t)$, $\hat{\theta}_2(t)$ and $\hat{\theta}_3(t)$, and the two feedback functions $m_1(x,t)$ and $m_2(x,t)$, in order to stabilize the error dynamics in (11)-(15).

The first step in the design is to decouple the PDE estimation errors $(\tilde{u}(x,t),\tilde{v}(x,t))$ from the ODE estimation error $\tilde{X}(t)$ and from the parameters estimation errors $\tilde{\theta}_1(t)$, $\tilde{\theta}_2(t)$ and $\tilde{\theta}_3(t)$. This is done using the swapping design method.

### *3.1 Swapping design*

The idea of the swapping design method is to write the PDE estimation errors $(\tilde{u}(x,t),\tilde{v}(x,t))$ as a linear combination of the ODE estimation error $\tilde{X}(t)$ and the parameters estimation errors $\tilde{\theta}_1(t)$, $\tilde{\theta}_2(t)$ and $\tilde{\theta}_3(t)$ as follows:

$$E(x,t)=W(x,t)-T(x,t)\tilde{X}(t)-R(x,t)\tilde{\theta}(t)\tag{16}$$

where $W(x,t)=\big(w_1(x,t),w_2(x,t)\big)^\top$, $E(x,t)=\big(\tilde{u}(x,t),\tilde{v}(x,t)\big)^\top$, $\tilde{\theta}(t)=\big(\tilde{\theta}_1(t),\tilde{\theta}_2(t),\tilde{\theta}_3(t)\big)^\top$, $T(x,t)=\big(T_1(x,t),T_2(x,t)\big)^\top$ and

$$R(x,t)=\begin{bmatrix}R_{11}(x,t)\ R_{12}(x,t)\ R_{13}(x,t)\\R_{21}(x,t)\ R_{22}(x,t)\ R_{23}(x,t)\end{bmatrix}.$$

$w_1(x,t)$ and $w_2(x,t)$ are two PDEs to be defined later. $T_1(x,t)$ and $T_2(x,t):[0,1]\times[0,+\infty)\to\mathbb{R}^{1\times n_X}$ are the swapping filters of the ODE estimation error $\tilde{X}(t)$. $R_{11}(x,t)$ and $R_{21}(x,t):[0,1]\times[0,+\infty)\to\mathbb{R}^{1\times n_{\theta_1}}$, $R_{12}(x,t)$ and $R_{22}(x,t):[0,1]\times[0,+\infty)\to\mathbb{R}^{1\times n_{\theta_2}}$, $R_{13}(x,t)$ and $R_{23}(x,t):[0,1]\times[0,+\infty)\to\mathbb{R}^{1\times n_{\theta_3}}$ are the swapping filters of the parameter estimation errors $\tilde{\theta}_1(t)$, $\tilde{\theta}_2(t)$ and $\tilde{\theta}_3(t)$, respectively. By substituting (11)-(15) in (16), one can verify that the systems $W(x,t)$, $T(x,t)$ and $R(x,t)$ obey the following set of partial differential equations:

$$W(x,t):\begin{cases}\partial_t w_1(x,t)+\lambda_1(x)\partial_x w_1(x,t)=\sigma_1(x)w_2(x,t)\\-p_1(x)w_1(1,t)\\\partial_t w_2(x,t)-\lambda_2(x)\partial_x w_2(x,t)=\sigma_2(x)w_1(x,t)\\-p_2(x)w_1(1,t)\\w_1(0,t)=qw_2(0,t),\quad w_2(1,t)=0\end{cases}\tag{17}$$

$$T(x,t):\begin{cases}\partial_t T_1(x,t)+\lambda_1(x)\partial_x T_1(x,t)=\sigma_1(x)T_2(x,t)\\-p_1(x)T_1(1,t)-T_1(x,t)A(t)\\\partial_t T_2(x,t)-\lambda_2(x)\partial_x T_2(x,t)=\sigma_2(x)T_1(x,t)\\-p_2(x)T_1(1,t)-T_2(x,t)A(t)\\T_1(0,t)=qT_2(0,t)-C,\quad T_2(1,t)=0\end{cases}\tag{18}$$

$$R_1(x,t):\begin{cases}\partial_t R_{11}(x,t)+\lambda_1(x)\partial_x R_{11}(x,t)=\\ \sigma_1(x)R_{21}(x,t)-p_1(x)R_{11}(1,t)-\phi_1(x,t)\\ \partial_t R_{21}(x,t)-\lambda_2(x)\partial_x R_{21}(x,t)=\\ \sigma_2(x)R_{11}(x,t)-p_2(x)R_{11}(1,t)\\ R_{11}(0,t)=qR_{21}(0,t),\quad R_{21}(1,t)=0\end{cases} \tag{19}$$

$$R_2(x,t):\begin{cases}\partial_t R_{12}(x,t)+\lambda_1(x)\partial_x R_{12}(x,t)=\\ \sigma_1(x)R_{22}(x,t)-p_1(x)R_{12}(1,t)\\ \partial_t R_{22}(x,t)-\lambda_2(x)\partial_x R_{22}(x,t)=\\ \sigma_2(x)R_{12}(x,t)-p_2(x)R_{12}(1,t)-\phi_2(x,t)\\ R_{12}(0,t)=qR_{22}(0,t),\quad R_{22}(1,t)=0\end{cases} \tag{20}$$

$$R_3(x,t):\begin{cases}\partial_t R_{13}(x,t)+\lambda_1(x)\partial_x R_{13}(x,t)=\\ \sigma_1(x)R_{23}(x,t)-p_1(x)R_{13}(1,t)-T_1(x,t)\psi(t)\\ \partial_t R_{23}(x,t)-\lambda_2(x)\partial_x R_{23}(x,t)=\\ \sigma_2(x)R_{13}(x,t)-p_2(x)R_{13}(1,t)-T_2(x,t)\psi(t)\\ R_{13}(0,t)=qR_{23}(0,t),\quad R_{23}(1,t)=0\end{cases} \tag{21}$$

with the following gains:

$$p_{y_1}(x,t)=p_1(x)-T_1(x,t)L(t), \tag{22}$$
$$p_{y_2}(x,t)=T_1(x,t)D(t) \tag{23}$$
$$r_{y_1}(x,t)=p_2(x)-T_2(x,t)L(t) \tag{24}$$
$$r_{y_2}(x,t)=T_2(x,t)D(t) \tag{25}$$
$$m(x,t)=-R(x,t)\dot{\hat{\theta}}(t) \tag{26}$$

where $m(x,t)=(m_1(x,t),m_2(x,t))^\top$. $p_1(x)$ and $p_2(x)$ are the static observer gains on the PDE side (to be determined later). We can infer from (16) that the PDE estimation error $E(x,t)$ is the sum of three errors: 1) $W(x,t)$, which is the estimation error due to the unknown initial conditions ($u_0(x)$,$v_0(x)$) of the plant (1)-(5). 2) $T(x,t)\tilde{X}(t)$, which is proportional to the ODEs estimation error $\tilde{X}(t)$ and 3) $R(x,t)\tilde{\theta}(t)$, which is proportional to the parameters estimation errors $\tilde{\theta}(t)$. The goal is to find the observer gains $p_1(x)$, $p_2(x)$ and $L(t)$ that drive the estimation error to zero. In fact, we aim to obtain sufficient conditions that can guarantee the exponential convergence of the error in the $\left|\tilde{X}\right|^2+\left|\tilde{\theta}\right|^2+||E(.,t)||^2_{(\mathbb{L}^2([0,1]))^2}$ norm. This norm is simply the sum of the $L^2$ norms of the PDEs and of the ODEs. From (16), in order to prove the exponential convergence of the $\{E(x,t),\ \tilde{X}(t),\ \tilde{\theta}(t)\}$ system, it is sufficient to prove the exponential convergence of the $\{W(x,t),\ \tilde{X}(t),\ \tilde{\theta}(t)\}$ system and the boundedness of the filters $T(x,t)$ and $R(x,t)$. Before starting the error stability analysis of the $\{W(x,t),\ \tilde{X}(t),\ \tilde{\theta}(t)\}$ system, we first analyze the dynamics of $\tilde{X}(t)$ and define the adaptive laws for estimating the parameters $\theta_1$, $\theta_2$ and $\theta_3$.

### *3.2 ODE error dynamics and the parameter estimation laws*

We evaluate (16) at $x=1$ and $x=0$, then substitute $\tilde{v}(0,t)$ and $\tilde{u}(1,t)$ in (15) to obtain:

$$\begin{aligned}\dot{\tilde{X}}(t)=&\Big(A(t)+K(t)\tilde{T}(t)\Big)\tilde{X}(t)-K(t)\tilde{w}(t)\\&+\Big(K(t)\Phi(t)+\Psi(t)\Big)\tilde{\theta}(t)\end{aligned} \tag{27}$$

where $K(t)=(L(t),-D(t))$, $\tilde{w}(t)=(w_1(1,t),w_2(0,t))^\top$, $\tilde{T}(t)=(T_1(1,t),T_2(0,t))^\top$,
$\Psi(t)=[0_{n_X\times n_{\theta_1}}\quad 0_{n_X\times n_{\theta_2}}\quad \psi(t)]$ and

$$\Phi(t)=\begin{bmatrix}R_{11}(1,t)\ R_{12}(1,t)\ R_{13}(1,t)\\ R_{21}(0,t)\ R_{22}(0,t)\ R_{23}(0,t)\end{bmatrix}.$$

For the parameters updates, after evaluating (16) at $x=1$ and $x=0$, and using the superposition principle (i.e. fixing $\tilde{w}=0$ and $\tilde{X}(t)=0$) we obtain the following linear regressor equation

$$\tilde{y}(t)=-\Phi(t)\tilde{\theta}(t) \tag{28}$$

which relates the estimation error $\tilde{y}(t)=\big(\tilde{u}(1,t),\tilde{v}(0,t)\big)^\top$ at the boundary to the parameter estimation errors $\tilde{\theta}(t)$, weighted by the regressor $\Phi(t)$. Equation (28) suggests the following normalized parameter adaptation algorithm:

$$\dot{\hat{\theta}}(t)=-\dot{\tilde{\theta}}(t)=-\frac{P_\theta(t)\Phi^\top(t)}{1+||\Phi^\top(t)\Phi(t)||^2}\tilde{y}(t) \tag{29}$$

$$\dot{P}_\theta(t)=\beta P_\theta(t)-\frac{P_\theta(t)\Phi^\top(t)\Phi(t)P_\theta(t)}{1+||\Phi^\top(t)\Phi(t)||^2} \tag{30}$$

where $P_\theta(t)$: $[0,+\infty)\longmapsto\mathbb{R}^{n_\theta\times n_\theta}$ with $n_\theta=n_{\theta_1}+n_{\theta_2}+n_{\theta_3}$ and $\beta>0$ is the forgetting factor. The initial conditions $\hat{\theta}(0)=\hat{\theta}_0$ and $P_\theta(0)$=$P_{\theta,0}$=$P^T_{\theta,0}$ are chosen arbitrarily. The adaptive law (29)-(30) is a continuous-time recursive least square estimator with a forgetting factor (see [19] for various linear regression estimation techniques). Now, we compute the dynamics of $\tilde{\theta}(t)$ in the ($W(x,t)$, $\tilde{X}(t)$, $\tilde{\theta}$) variables by inserting (16) into (29):

$$\begin{aligned}\dot{\tilde{\theta}}(t)=\frac{P_\theta(t)}{1+||\Phi^\top(t)\Phi(t)||^2}\Big[&-\Phi^\top(t)\Phi(t)\tilde{\theta}(t)\\&-\Phi^\top(t)\tilde{T}(t)\tilde{X}(t)+\Phi^\top(t)\tilde{w}(t)\Big].\end{aligned} \tag{31}$$

Note that (27) and (31) are coupled with the PDEs of the $W(x,t)$ system at the right boundary $x=1$ through $w_1(x,t)$ and at the left boundary $x=0$ through $w_2(0,t)$.

However, the $W(x,t)$ system in (17) is totally decoupled from the ODE dynamics. This is because $W(x,t)$ is the error due to the unknown initial conditions of the PDE plant $\{u(x,t), v(x,t)\}$. This estimation error is always present independently from the ODE states and the parameters.

The observer gains $p_1(x)$, $p_2(x)$ and $L(t)$ are designed to guarantee the exponential convergence of the error system $\{E(x,t),\ \tilde{X}(t),\ \tilde{\theta}(t)\}$ in the $\left|\tilde{X}\right|^2+\left|\tilde{\theta}\right|^2+ ||E(.,t)||^2_{(\mathbb{L}^2([0,1]))^2}$ norm. For this design, we first study the stability of the decoupled $W(x,t)$ system, then the boundedness of the filters $T(x,t)$ and $R(x,t)$ and finally the stability of the $\{W(x,t),\ \tilde{X}(t),\ \tilde{\theta}(t)\}$ system. After these steps, the stability of the $\{E(x,t),\ \tilde{X}(t),\ \tilde{\theta}(t)\}$ system is easily deduced from (16), as shown in the next sections.

### *3.3 Stability of the $W(x,t)$ system*

The problem of finding the gains $p_1(x)$ and $p_2(x)$ that stabilize the $W(x,t)$ system is solved by [23]. We recall these results here, adapted to our framework. Using an invertible Volterra backstepping transformation, $W(x,t)$ is mapped into a stable target system $\Gamma(x,t) = (\gamma_1(x,t), \gamma_2(x,t))^T$:

$$\Gamma(x,t): \begin{cases} \partial_t \gamma_1(x,t) + \lambda_1(x)\partial_x \gamma_1(x,t) = 0 \\ \partial_t \gamma_2(x,t) - \lambda_2(x)\partial_x \gamma_2(x,t) = 0 \\ \gamma_1(0,t) = q\gamma_2(0,t) \\ \gamma_2(1,t) = 0 \end{cases} \tag{32}$$

The $\Gamma(x,t)$ system is a cascade stable system. The PDE in $\gamma_2(x,t)$ is decoupled from $\gamma_1(x,t)$ and has a zero boundary condition at $x=1$. $\gamma_2(x,t)$ converges to zero after the transport time $t_{F2} = \int_0^1 \frac{1}{\lambda_2(x)}dx$ is passed. After the time $t_{F2}$, $\gamma_1(x,t)$ has a zero boundary condition at $x=0$ and it takes a time $t_{F1} = \int_0^1 \frac{1}{\lambda_1(x)}dx$ to converge to zero. So the system $\Gamma(x,t)$ converges to zero ($\gamma_1 = \gamma_2 = 0$) in a finite-time equals to $t_F = t_{F1} + t_{F2}$. One can also show, using a quadratic Lyapunov function of the form $V(t) = \int_0^1 \left(q_1\gamma_1^2(x,t) + q_2\gamma_2^2(x,t)\right)dx$, $q_1 > 0$ and $q_2 > 0$, that the $\Gamma(x,t)$ system is exponentially stable in the $||\Gamma(.,t)||^2_{(\mathbb{L}^2([0,1]))^2}$ norm. Therefore, $\Gamma(x,t)$ is exponentially stable in the $L^2$ norm and its equilibrium ($\gamma_1 = \gamma_2 = 0$) is reached in a finite time equals to $t_F$. These stability characteristics are transferred to the $W(x,t)$ system by the invertibility of the backstepping transformation. The backstepping transformations that map $W(x,t)$ into $\Gamma(x,t)$ and vice-versa are [23]:

$$W(x,t) = \Gamma(x,t) - \int_x^1 P_*(x,\xi)\Gamma(\xi,t)d\xi \tag{33}$$

$$\Gamma(x,t) = W(x,t) + \int_x^1 R_*(x,\xi)W(\xi,t)d\xi \tag{34}$$

with

$$P_*(x,\xi) = \begin{bmatrix} P_*^{11}(x,\xi) & P_*^{12}(x,\xi) \\ P_*^{21}(x,\xi) & P_*^{22}(x,\xi) \end{bmatrix}$$

$$R_*(x,\xi) = \begin{bmatrix} R_*^{11}(x,\xi) & R_*^{12}(x,\xi) \\ R_*^{21}(x,\xi) & R_*^{22}(x,\xi) \end{bmatrix}.$$

$P_*(x,\xi)$ is called the direct backstepping kernel and $R_*(x,\xi)$ is called the inverse backstepping kernel. Both kernels are defined on the triangular domain $\mathbb{L} = \{(x,\xi), 0 \le x \le \xi \le 1\}$. The equations of $P_*(x,\xi)$ and $R_*(x,\xi)$ are defined in [23] (more precisely equations (67)-(74) for $P_*(x,\xi)$ and equations (81)-(88) for $R_*(x,\xi)$ in [23]). The observer gains are derived from the equations of $P_*(x,\xi)$ as:

$$\begin{aligned} p_1(x) &= -\lambda_1(1)P_*^{11}(x,1), \\ p_2(x) &= -\lambda_1(1)P_*^{21}(x,1) \end{aligned} \tag{35}$$

The couplings $\sigma_1(x)$, $\sigma_2(x)$ and $q$ are encapsulated in $P_*(x,\xi)$, which is the base for calculating the observer gains $p_1(x)$ and $p_2(x)$ in (35). The observer gains cancel the effects of the couplings and allow the transformation from $W(x,t)$ to $\Gamma(x,t)$. Finally, the stability of the $W(x,t)$ system is summarized by the following theorem.

**Theorem 1 ([23])** *Consider the system $W(x,t)$ system in (17) with initial conditions $w_1^0, w_2^0$ in $\mathbb{L}^2[0,1]$ and with observer gains (35). The equilibrium $w_1 \equiv w_2 \equiv 0$ is exponentially stable in the $L^2$ sense, and the equilibrium is reached in finite time $t_F = \int_0^1 \left(\frac{1}{\lambda_1(x)} + \frac{1}{\lambda_2(x)}\right)dx$.*

### *3.4 Boundedness of the $T(x,t)$ and the $R(x,t)$ filters*

Since the filters $T(x,t)$ and $R(x,t)$ have the same coupling architecture, we first prove the boundedness of $T(x,t)$ (in the $L^2$ sense), then the boundedness of $R(x,t)$ follows exactly in the same way.

**Lemma 1** *The system $T(x,t)$ is mapped by the $R_*(x,\xi)$ inverse backstepping transformation to the following target system*

$$\eta(x,t): \begin{cases} \partial_t \eta_1(x,t) + \lambda_1(x)\partial_x \eta_1(x,t) = -\eta_1(x,t)A(t) \\ \partial_t \eta_2(x,t) - \lambda_2(x)\partial_x \eta_2(x,t) = -\eta_2(x,t)A(t) \\ \eta_1(0,t) = q\eta_2(0,t) - C, \quad \eta_2(1,t) = 0 \end{cases} \tag{36}$$

with $\eta_1(x,t)$ and $\eta_2(x,t) : [\,0,1\,] \times [\,0,+\infty) \to \mathbb{R}^{1\times n_X}$.

**PROOF.** We begin by writing the $T(x,t)$ and the $\eta(x,t)$ systems in the index format, for all $1 \le i \le n_X$:

$$\begin{cases} \partial_t T_1^i(x,t) + \lambda_1(x)\partial_x T_1^i(x,t) = \sigma_1(x) T_2^i(x,t) \\ -p_1(x) T_1^i(1,t) - \sum_{j=1}^{n_X} T_1^j(x,t) a_{ji}(t) \\ \partial_t T_2^i(x,t) - \lambda_2(x)\partial_x T_2^i(x,t) = \sigma_2(x) T_1^i(x,t) \\ -p_2(x) T_1^i(1,t) - \sum_{j=1}^{n_X} T_2^j(x,t) a_{ji}(t) \\ T_1^i(0,t) = q T_2^i(0,t) - c_i, \quad T_2^i(1,t) = 0 \end{cases} \tag{37}$$

$$\begin{cases} \partial_t \eta_1^i(x,t) + \lambda_1(x)\partial_x \eta_1^i(x,t) = -\sum_{j=1}^{n_X} \eta_1^j(x,t) a_{ji}(t) \\ \partial_t \eta_2^i(x,t) - \lambda_2(x)\partial_x \eta_2^i(x,t) = -\sum_{j=1}^{n_X} \eta_2^j(x,t) a_{ji}(t) \\ \eta_1^i(0,t) = q \eta_2^i(0,t) - c_i, \quad \eta_2^i(1,t) = 0 \end{cases} \tag{38}$$

The transformation that maps $T^i(x,t)$ into $\eta^i(x,t)$ is

$$\begin{aligned} \eta_1^i(x,t) = T_1^i(x,t) &+ \int_x^1 R_*^{11}(x,\xi) T_1^i(\xi,t) d\xi \\ &+ \int_x^1 R_*^{12}(x,\xi) T_2^i(\xi,t) d\xi \end{aligned} \tag{39}$$

$$\begin{aligned} \eta_2^i(x,t) = T_2^i(x,t) &+ \int_x^1 R_*^{21}(x,\xi) T_1^i(\xi,t) d\xi \\ &+ \int_x^1 R_*^{22}(x,\xi) T_2^i(\xi,t) d\xi \end{aligned} \tag{40}$$

This transformation is obtained by differentiating (39) and (40) with respect to time, replacing them in (37), then integrating by parts to get

$$\begin{aligned} &\partial_t \eta_1^i(x,t) = -\lambda_1(x)\partial_x T_1^i(x,t) + \sigma_1(x) T_2^i(x,t) \\ &- \sum_{j=1}^{n_X} T_1^j(x,t) a_{ji}(t) - T_1^i(1,t)\Big[p_1(x) + \lambda_1(1) R_*^{11}(x,1) \\ &+ \int_x^1 \big[p_1(\xi) R_*^{11}(x,\xi) + p_2(\xi) R_*^{12}(x,\xi)\big] d\xi\Big] \\ &+ \lambda_1(x) R_*^{11}(x,x) T_1^i(x,t) + \big(\sigma_1(x) - \lambda_2(x) R_*^{12}(x,x)\big) T_2^i(x,t) \\ &+ \int_x^1 \Big[\lambda_1'(\xi) R_*^{11}(x,\xi) + \lambda_1(\xi)\partial_\xi R_*^{11}(x,\xi) \\ &+ \sigma_2(\xi) R_*^{12}(x,\xi)\Big] T_1^i(\xi,t) d\xi - \int_x^1 \Big[\lambda_2'(\xi) R_*^{12}(x,\xi) \\ &+ \lambda_2(\xi)\partial_\xi R_*^{12}(x,\xi) - \sigma_1(\xi) R_*^{11}(x,\xi)\Big] T_2^i(\xi,t) d\xi \\ &- \int_1^x \sum_{j=1}^{n_X} \Big[R_*^{11}(x,\xi) T_1^j(\xi,t) + R_*^{12}(x,\xi) T_2^j(\xi,t)\Big] a_{ji}(t) d\xi \end{aligned} \tag{41}$$

$$\begin{aligned} &\partial_t \eta_2^i(x,t) = \lambda_2(x)\partial_x T_2^i(x,t) + \sigma_2(x) T_1^i(x,t) \\ &- \sum_{j=1}^{n_X} T_2^j(x,t) a_{ji}(t) - T_1^i(1,t)\Big[p_2(x) + \lambda_1(1) R_*^{21}(x,1) \\ &+ \int_x^1 \big[p_1(\xi) R_*^{21}(x,\xi) + p_2(\xi) R_*^{22}(x,\xi)\big] d\xi\Big] \\ &+ \big(\lambda_1(x) R_*^{21}(x,x) + \sigma_2(x)\big) T_1^i(x,t) - \lambda_2(x) R_*^{22}(x,x) T_2^i(x,t) \\ &+ \int_x^1 \Big[\lambda_1'(\xi) R_*^{21}(x,\xi) + \lambda_1(\xi)\partial_\xi R_*^{21}(x,\xi) \\ &+ \sigma_2(\xi) R_*^{22}(x,\xi)\Big] T_1^i(\xi,t) d\xi - \int_x^1 \Big[\lambda_2'(\xi) R_*^{22}(x,\xi) \\ &+ \lambda_2(\xi)\partial_\xi R_*^{22}(x,\xi) - \sigma_1(\xi) R_*^{21}(x,\xi)\Big] T_2^i(\xi,t) d\xi \\ &- \int_1^x \sum_{j=1}^{n_X} \Big[R_*^{21}(x,\xi) T_1^j(\xi,t) + R_*^{22}(x,\xi) T_2^j(\xi,t)\Big] a_{ji}(t) d\xi \end{aligned} \tag{42}$$

Differentiating (39) and (40) with respect to space, then substituting them in (38), we get

$$\begin{aligned} &\partial_t \eta_1^i(x,t) = -\lambda_1(x)\Big[\partial_x T_1^i(x,t) - R_*^{11}(x,x) T_1^i(x,t) \\ &- R_*^{12}(x,x) T_2^i(x,t) + \int_x^1 \partial_x R_*^{11}(x,\xi) T_1^i(\xi,t) d\xi \\ &+ \int_x^1 \partial_x R_*^{12}(x,\xi) T_2^i(\xi,t) d\xi\Big] - \sum_{j=1}^{n_X} T_1^j(x,t) a_{ji}(t) \\ &- \int_1^x \sum_{j=1}^{n_X} \Big[R_*^{11}(x,\xi) T_1^j(\xi,t) + R_*^{12}(x,\xi) T_2^j(\xi,t)\Big] a_{ji}(t) d\xi \end{aligned} \tag{43}$$

$$\begin{aligned} &\partial_t \eta_2^i(x,t) = \lambda_2(x)\Big[\partial_x T_2^i(x,t) - R_*^{21}(x,x) T_1^i(x,t) \\ &- R_*^{22}(x,x) T_2^i(x,t) + \int_x^1 \partial_x R_*^{21}(x,\xi) T_1^i(\xi,t) d\xi \\ &+ \int_x^1 \partial_x R_*^{22}(x,\xi) T_2^i(\xi,t) d\xi\Big] - \sum_{j=1}^{n_X} T_2^j(x,t) a_{ji}(t) \\ &- \int_1^x \sum_{j=1}^{n_X} \Big[R_*^{21}(x,\xi) T_1^j(\xi,t) + R_*^{22}(x,\xi) T_2^j(\xi,t)\Big] a_{ji}(t) d\xi \end{aligned} \tag{44}$$

By equalizing (41) to (43) and (42) to (44) and substituting the boundary conditions at $x = 0$, one directly obtain the kernel equations (81)-(88) for $R_*(x,\xi)$ in [23]. The terms multiplying $T_1^i(1,t)$ in (41) and (42) cancel out using (35) and the relation between the direct kernel $P_*(x,\xi)$ and the inverse kernel $R_*(x,\xi)$ given by:

$$P_*(x,\xi) = R_*(x,\xi) - \int_x^\xi R_*(x,y) P_*(y,\xi) dy \tag{45}$$

Since the $\eta(x,t)$ system and the $T(x,t)$ system have the same boundedness properties by the invertibility of the backstepping transformation (39)-(40), we study the $L^2$ boundedness of the $\eta(x,t)$ system in the $L^2$ sense and deduce the boundedness of the $T(x,t)$ system. This is inferred from the following Theorem.

**Theorem 2** *Consider the $T(x,t)$ system in* (18)*. If $A(t)$ is bounded for all $t$, i.e. if there exist $M > 0$ such that $|a_{ij}(t)| \leq M$ for all $1 \leq i \leq n_X$, $1 \leq j \leq n_X$, then $T(x,t)$ is bounded in the $L^2$ sense.*

**PROOF.** Consider the $\eta(x,t)$ system in (36). We define the following quadratic Lyapunov function

$$V_1(t) = \int_0^1 \Big[\eta_1(x,t)Q_1 e^{-\mu x}\eta_1^\top(x,t) + \eta_2(x,t)Q_2 e^{\mu x}\eta_2^\top(x,t)\Big]dx \tag{46}$$

which is the weighted $L^2$ norm of $\eta(x,t)$. $Q_1$ and $Q_2$ are two positive definite matrices which are diagonal. $\mu > 0$ is a strictly positive constant. Taking the time derivative of (46) then substituting into (36) implies that:

$$\begin{aligned}\dot{V}_1(t) = &\int_0^1 -\lambda_1(x)\Big[\partial_x\eta_1(x,t)Q_1e^{-\mu x}\eta_1^\top(x,t) \\ &+ \eta_1(x,t)Q_1e^{-\mu x}\partial_x\eta_1^\top(x,t)\Big]dx - \int_0^1 \eta_1(x,t)\Big[ \\ &A(t)Q_1e^{-\mu x} + Q_1e^{-\mu x}A^\top(t)\Big]\eta_1^\top(x,t)dx \\ &+ \int_0^1 \lambda_2(x)\Big[\partial_x\eta_2(x,t)Q_2e^{\mu x}\eta_2^\top(x,t)+ \\ &\eta_2(x,t)Q_2e^{\mu x}\partial_x\eta_2^\top(x,t)\Big]dx - \int_0^1 \eta_2(x,t)\Big[ \\ &A(t)Q_2e^{\mu x} + Q_2e^{\mu x}A^\top(t)\Big]\eta_2^\top(x,t)dx\end{aligned}$$

Integration by parts and substitution of the boundary conditions of (36) gives:

$$\begin{aligned}\dot{V}_1(t) = &-\lambda_1(1)\eta_1(1,t)Q_1e^{-\mu}\eta_1^\top(1,t) \\ &- \lambda_2(0)\eta_2(0,t)Q_2\eta_2^\top(0,t) \\ &+ \lambda_1(0)\big(q\eta_2(0,t) - C\big)Q_1\big(q\eta_2^\top(0,t) - C^\top\big) \\ &+ \int_0^1 \eta_1(x,t)\Big[\lambda_1'(x)Q_1 - \mu\lambda_1(x)Q_1 - A(t)Q_1 \\ &- Q_1A^\top(t)\Big]e^{-\mu x}\eta_1^\top(x,t)dx + \int_0^1 \eta_2(x,t)\Big[ - \lambda_2'(x)Q_2 \\ &- \mu\lambda_2(x)Q_2 - A(t)Q_2 - Q_2A^\top(t)\Big]e^{\mu x}\eta_2^\top(x,t)dx\end{aligned} \tag{47}$$

As $A(t)$ is bounded for all $t$ and $\lambda_1(x)$, $\lambda_2(x)$ are sufficiently smooth on $[0,1]$, then for a $\mu$ large enough, there exists $\alpha_\eta > 0$ such that

$$\lambda_1'(x)Q_1 - \mu\lambda_1(x)Q_1 - A(t)Q_1 - Q_1A^\top(t) \leq -\alpha_\eta Q_1 \tag{48}$$

$$-\lambda_2'(x)Q_2 - \mu\lambda_2(x)Q_2 - A(t)Q_2 - Q_2A^\top(t) \leq -\alpha_\eta Q_2 \tag{49}$$

By applying Young's inequality to the third term of (47), and using (48)-(49), one obtains

$$\begin{aligned}\dot{V}_1(t) \leq &\ \eta_2(0,t)\Big[ - \lambda_2(0)Q_2 + \lambda_1(0)q(1+q)Q_1\Big]\eta_2^\top(0,t) \\ &+ (1+q)\lambda_1(0)CQ_1C^\top - \alpha_\eta V_1(t)\end{aligned} \tag{50}$$

Now, choosing the diagonal positive matrices $Q_1$ and $Q_2$ such that

$$Q_1 \leq \frac{\lambda_2(0)}{\lambda_1(0)q(1+q)}Q_2 \tag{51}$$

to have the first term of (50) negative, we obtain

$$\dot{V}_1(t) \leq -\alpha_\eta V_1(t) + (1+q)\lambda_1(0)CQ_1C^\top \tag{52}$$

It follows from (52) that $V_1(t)$ is bounded. Since $V_1(t)$ is the weighted $L^2$ norm of $\eta(x,t)$, then $\eta(x,t)$ is bounded in the $L^2$ sense. Now by the invertibility of the backstepping transformation (39)-(40), $T(x,t)$ is bounded in the $L^2$ sense and the proof is complete.

**Remark 1** *The boundedness of the $R(x,t)$ filters is done in the same way. The first step is to set the suitable target systems to decouple the system $R(x,t)$ using the backstepping transformation* (39)-(40)*. Then we define a quadratic Lyapunov function similar to* (46) *to obtain the $L^2$ boundedness.*

### *3.5 Stability of the $\{W(x,t),\ \tilde{X}(t),\ \tilde{\theta}(t)\}$ system*

In this section we give sufficient conditions that guarantee the $L^2$ stability of the $\{W(x,t),\ \tilde{X}(t),\ \tilde{\theta}(t)\}$ system. This is the last step before concluding on the stability of the $\{E(x,t),\ \tilde{X}(t),\ \tilde{\theta}(t)\}$ system. The static observer gains $p_1(x)$ and $p_2(x)$ are calculated in (35). Now, we give the method for calculating the time varying observer gain $L(t)$.

We start by writing the ODE estimation error dynamics $\tilde{X}(t)$ in (27) and the parameter estimation error dynamics $\tilde{\theta}(t)$ in (31) in the matrix form as

$$\begin{bmatrix}\dot{\tilde{X}}(t)\\ \dot{\tilde{\theta}}(t)\end{bmatrix} = A_c(t)\begin{bmatrix}\tilde{X}(t)\\ \tilde{\theta}(t)\end{bmatrix} + B_c(t)\tilde{w}(t) \tag{53}$$

where:

$$A_c(t) = \begin{bmatrix} A(t) + K(t)\tilde{T}(t) & K(t)\Phi(t) + \Psi(t) \\ -\dfrac{P_\theta(t)\Phi^\top(t)\tilde{T}(t)}{1+||\Phi^\top(t)\Phi(t)||^2} & -\dfrac{P_\theta(t)\Phi^\top(t)\Phi(t)}{1+||\Phi^\top(t)\Phi(t)||^2} \end{bmatrix},$$

$$B_c(t) = \begin{bmatrix} -K(t) \\ \dfrac{P_\theta(t)\Phi^\top(t)}{1+||\Phi^\top(t)\Phi(t)||^2} \end{bmatrix}$$

Notice that the PDE dynamics of $W(x,t)$ in (17) interfere with the ODEs through the matrix $B_c(t)$, which is multiplied by the output $\tilde{w}(t)$ of the $W(x,t)$ system. This is interesting because the $W(x,t)$ system is finite-time converging by Theorem 1, i.e. $\tilde{w}(t)$ is equal to zero for $t \geq t_F$. After the total transport time $t_F$, the PDE and the ODE estimation errors are thus totally decoupled from each other. Using the filters design in (16) along with the choice of the shape of the time varying observer gains $p(x,t) = (p_{y_1}(x,t), p_{y_2}(x,t))^\top$ and $r(x,t) = (r_{y_1}(x,t), r_{y_2}(x,t))^\top$ in (22)-(24), the ODE dynamics (53) becomes a simple linear time varying system with a state matrix $A_c(t)$. The stability of the $\{W(x,t), \tilde{X}(t), \tilde{\theta}(t)\}$ system is thus determined with respect to the characteristics of the matrix $A_c(t)$ after the time $t_F$, as shown in the following theorem.

**Theorem 3** *Consider the system* (17) *and* (53)*. If* $\Phi(t)$ *is bounded and persistently exciting (PE), i.e. for all* $t \geq t_F$ *there exist positive constants* $T_0$*,* $c_0$ *and* $c_1$ *so that:*

$$c_0 I \leq \int_t^{t+T_0} \Phi^\top(\tau)\Phi(\tau)d\tau \leq c_1 I \tag{54}$$

*In addition, if there exist an observer gain* $L(t) \in \mathbb{R}^{n_X \times 1}$ *and a bounded matrix* $P_X(t) \in S_+^{n_X \times n_X}$ *such that, for all* $t \geq t_F$*:*

$$Z(t) \leq -Q \tag{55}$$

*where* $Z(t)$ *is a symmetric matrix with entities*

$$\begin{aligned} Z_{11}(t) &= \dot{P}_X(t) + \big(A(t) + K(t)\tilde{T}(t)\big)^\top P_X(t) \\ &\quad + P_X(t)\big(A(t) + K(t)\tilde{T}(t)\big) \\ Z_{12}(t) &= P_X(t)\big(K(t)\Phi(t) + \Psi(t)\big) - \frac{\tilde{T}^\top(t)\Phi(t)}{1+||\Phi^\top(t)\Phi(t)||^2} \\ Z_{21}(t) &= Z_{12}^\top(t) \\ Z_{22}(t) &= -\beta P_\theta^{-1}(t) - \frac{\Phi^\top(t)\Phi(t)}{1+||\Phi^\top(t)\Phi(t)||^2} \end{aligned}$$

*and* $Q$ *is a predefined positive definite matrix. Then for all* $t \geq t_F$*, the system* $\{W(x,t), \tilde{X}(t), \tilde{\theta}(t)\}$ *is exponentially stable in the* $|\tilde{X}|^2 + |\tilde{\theta}|^2 + ||W(.,t)||^2_{(\mathbb{L}^2([0,1]))^2}$ *norm.*

**PROOF.** Define the Lyapunov function

$$\begin{aligned} V_2(t) &= \tilde{X}^\top(t)P_X(t)\tilde{X}(t) + \tilde{\theta}^\top(t)P_\theta^{-1}(t)\tilde{\theta}(t) \\ &\quad + ||W(.,t)||^2_{(\mathbb{L}^2([0,1]))^2} \end{aligned} \tag{56}$$

where $P_X(t)$ is a positive definite matrix related to $\tilde{X}(t)$ and $P_\theta^{-1}(t)$ is the inverse of $P_\theta(t)$ in (30). The authors in [19] have shown that if the regressor $\Phi(t)$ is bounded and persistently exciting i.e. if condition (54) is satisfied, then $P_\theta^{-1}(t)$ exists and it is positive definite and bounded for all $t \geq 0$. In this case, the dynamics of $P_\theta^{-1}(t)$ are calculated from $P_\theta(t)$ in (30) as

$$\frac{d}{dt}P_\theta^{-1}(t) = -\beta P_\theta^{-1}(t) + \frac{\Phi^\top(t)\Phi(t)}{1+||\Phi^\top(t)\Phi(t)||^2} \tag{57}$$

Now we differentiate (56) with respect to time and then substitute (53) and (57) to obtain

$$\begin{aligned} \dot{V}_2(t) &= \tilde{X}^\top(t)\Big[\dot{P}_X(t) + \Big(A(t) + K(t)\tilde{T}(t)\Big)^\top P_X(t) \\ &\quad + P_X(t)\Big(A(t) + K(t)\tilde{T}(t)\Big)\Big]\tilde{X}(t) + \tilde{\theta}^\top(t)\Big[-\beta P_\theta^{-1}(t) \\ &\quad - \frac{\Phi^\top(t)\Phi(t)}{1+||\Phi^\top(t)\Phi(t)||^2}\Big]\tilde{\theta}(t) + \tilde{X}^\top(t)\Big[P_X(t)\Big(K(t)\Phi(t) \\ &\quad + \Psi(t)\Big) - \frac{\tilde{T}^\top(t)\Phi(t)}{1+||\Phi^\top(t)\Phi(t)||^2}\Big]\tilde{\theta}(t) + \tilde{\theta}^\top(t)\Big[\Big(K(t)\Phi(t) \\ &\quad + \Psi(t)\Big)^\top P_X(t) - \frac{\Phi^T(t)\tilde{T}(t)}{1+||R_1^\top(t)R_1(t)||^2}\Big]\tilde{X}(t) \\ &\quad - \tilde{w}^\top(t)K^\top(t)P_X(t)\tilde{X}(t) - \tilde{X}^\top(t)P_X(t)K(t)\tilde{w}(t) \\ &\quad + \tilde{w}^\top(t)\frac{\Phi(t)}{1+||\Phi^\top(t)\Phi(t)||^2}\tilde{\theta}(t) \\ &\quad + \tilde{\theta}^\top(t)\frac{\Phi^\top(t)}{1+||\Phi^\top(t)\Phi(t)||^2}\tilde{w}(t) + \frac{d}{dt}||W(.,t)||^2_{(\mathbb{L}^2([0,1]))^2} \end{aligned} \tag{58}$$

We have from Theorem 1 that $\tilde{w}(t) = 0$ for $t \geq t_F$, then (58) becomes, for $t \geq t_F$

$$\begin{aligned} \dot{V}_2(t) &= \begin{bmatrix} \tilde{X}(t) \\ \tilde{\theta}(t) \end{bmatrix}^\top \begin{bmatrix} Z_{11}(t) & Z_{12}(t) \\ Z_{21}(t) & Z_{22}(t) \end{bmatrix} \begin{bmatrix} \tilde{X}(t) \\ \tilde{\theta}(t) \end{bmatrix} \\ &\quad + \frac{d}{dt}||W(.,t)||^2_{(\mathbb{L}^2([0,1]))^2} \end{aligned} \tag{59}$$

If there exist $Q$ positive definite such that (55) is satisfied, and since $W(x,t)$ is exponentially decaying in the $L^2$ norm by Theorem 1, we have

$$\dot{V}_2(t) \leq -\begin{bmatrix} \tilde{X}(t) \\ \tilde{\theta}(t) \end{bmatrix}^\top Q \begin{bmatrix} \tilde{X}(t) \\ \tilde{\theta}(t) \end{bmatrix} - \alpha_W ||W(.,t)||^2_{(\mathbb{L}^2([0,1]))^2} \tag{60}$$

where $\alpha_W > 0$ is the rate of the exponential convergence of the $L^2$ norm of $W(x,t)$. By (60), there exists $\alpha > 0$ such that $\dot{V}_2(t) \leq -\alpha V_2(t)$ for all $t \geq t_f$. Since $V_2(t)$ is the weighted $L^2$ norm of the $\{W(x,t),\ \tilde{X}(t),\ \tilde{\theta}(t)\}$ system, then for all $t \geq t_F$ this system is exponentially stable in the $\left|\tilde{X}\right|^2 + \left|\tilde{\theta}\right|^2 + ||W(.,t)||^2_{(\mathbb{L}^2([0,1]))^2}$ norm and the proof is complete.

**Remark 2** *Since $Z(t)$ is a symmetric matrix, then there are two necessary conditions for* (55) *to have feasible solutions. The first one is that $Z_{11}(t)$ must be negative definite ($Z_{11}(t) \prec 0$). Note that $Z_{11}(t)$ is the differential Lyapunov equation in the matrix $A(t) + K(t)\tilde{T}(t)$. For $Z_{11}(t) \prec 0$ to be feasible, there must exist a positive definite matrix $P_X(t)$ such that $Z_{11}(t) \prec 0$. But $P_X(t)$ can only exist if the matrix $A(t) + K(t)\tilde{T}(t)$ is uniformly exponentially stable (UES). Any time-varying state matrix which is 1) continuously differentiable, 2) bounded, 3) slowly varying and 4) the real part of its eigen-values is negative for all times is UES (see e.g. Theorem 8.7 in [22]). For instance if we assume that $A(t)+K(t)\tilde{T}(t)$ satisfies the first three conditions of Theorem 8.7 in [22] in the interval of time $[t_F, +\infty)$, we also require that the real part of its eigenvalues is negative on this interval. Since we do not assume any conditions on the eigenvalues of $A(t)$, it is the role of the observer gain $L(t)$ to make the real part of the eigenvalues of $A(t) - D(t)T_2(0,t) + L(t)T_1(1,t)$ negative. This depends on the detectability of the pair $(A(t), C)$. To see this, one can notice from the system $T(x,t)$ in* (18) *or from its transform $\eta(x,t)$ in* (36) *that $\tilde{T}(t) = [T_1(1,t), T_2(0,t)]^\top$ is a time-delayed version of the output matrix $C$. If $C = 0$, then for $t \geq t_F$, $T(x,t) \equiv \eta(x,t) \equiv 0$, which makes $Z_{11}(t) \prec 0$ not feasible in the case where the ODE matrix $A(t)$ is not UES. This is what we mentioned early in the beginning of the Section 2. A second necessary condition for* (55) *is that $Z_{22}(t)$ has to be negative definite ($Z_{22}(t) \prec 0$), which is the case from the definition of the inverse matrix $P_\theta^{-1}(t)$. Note that the persistency of excitation* (54) *is satisfied if $\phi_1(x,t)$, $\phi_2(x,t)$ and $\psi(t)$ are persistently exciting (considering the definition of $\Phi(t)$ along with* (19), (20) *and* (21)*).*

We now state the stability results of the $\{E(x,t),\ \tilde{X}(t),\ \tilde{\theta}(t)\}$ system.

**Theorem 4** *Under Theorems 1-3, the system $\{E(x,t),\ \tilde{X}(t),\ \tilde{\theta}(t)\}$ is exponentially stable in the $V(t) = \left|\tilde{X}\right|^2 + \left|\tilde{\theta}\right|^2 + ||E(.,t)||^2_{(\mathbb{L}^2([0,1]))^2}$ norm for all $t \geq t_F$.*

**PROOF.** This result is straightforward from (16) and using the Theorems 1-3.

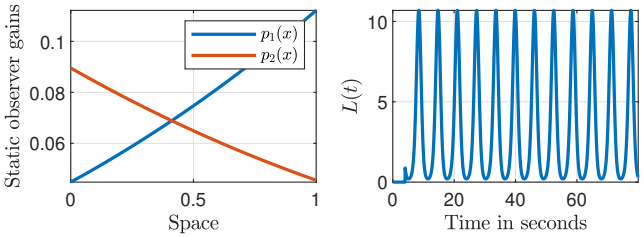


Fig. 3. Unstable plant: observer gains evolution

## 4 Numerical Simulations (Unstable plant)

The goal of this section is to analyze the performance of the adaptive observer (6)-(10) on an unstable plant. Consider the following toy parameters of model (1)-(5):

$$\begin{aligned}
\lambda_1(x) &= 0.6 + 0.1\sin(10x),\ U(t) = 1,\ \theta_1 = 1,\ \theta_2 = 5\\
\lambda_2(x) &= 0.4 + 0.1\sin(10x),\ V(t) = 1,\ \theta_3 = -5\\
\sigma_1(x) &= 0.3e^{0.9x},\ \sigma_2(x) = 0.2e^{-0.9x},\ \psi(t) = \cos(t)\\
\phi_1(x,t) &= 1 + \sin(10x)e^{-0.001t},\ A(t) = \sin(t),\ C = 1\\
\phi_2(x,t) &= 1 + \cos(10x)e^{-0.001t},\ B(t) = 1,\ D(t) = -1
\end{aligned}$$

This system is unstable because the matrix $A(t) = \sin(t)$ is not stable. We simulate the adaptive observer (6)-(10) in several steps. The first step is to compute the static observer gains $p_1(x)$ and $p_2(x)$ offline, by solving the kernel equations $P_*(x,\xi)$ using the method of successive approximations [18]. The main idea of this method is to write the set of PDEs of $P_*(x,\xi)$ in the integral form using the method of characteristics. Afterwards, the integral equations are solved using recursion up to an order of accuracy defined by the user. The gains $p_1(x) = -\lambda(1)P_*^{11}(x,1)$ and $p_2(x) = -\lambda_1(1)P_*^{21}(x,1)$ are plotted on Figure 3. The second step is to compute the filters $T(x,t)$ and $R(x,t)$. The dynamics of the filters (18)-(21) are discretized using finite difference schemes (Euler forward and backward schemes are used for space discretization and the explicit scheme is used for time discretization). The third step is to set the gains $\beta$ and $L(t)$. $\beta$ is the forgetting factor responsible for the speed of convergence of the parameter estimations and it is set to $\beta = 0.1$. The persistency of excitation condition (54) depends on the values of $\phi_1(x,t)$, $\phi_2(x,t)$ and $\psi(t)$. One pratical way to verify this condition is to look into the eigen values of the matrix $P_\theta(t)$ plotted on Figure 4. The eigen values remain strictly positive and this indicates that the regressor $\Phi(t)$ is persistently exciting for the chosen toy values of $\phi_1(x,t)$, $\phi_2(x,t)$ and $\psi(t)$.

The dynamic observer gain $L(t)$ is calculated at each time step to ensure that $Z(t)$ in (55) is negative definite for $t \geq t_F = \int_0^1 \left(\frac{1}{\lambda_1(x)} + \frac{1}{\lambda_2(x)}\right)dx \approx 4\,s$. This is done in the following order: 1) use a pole placement method to compute $L(t)$ that guarantees the existence of $P_X(t)$

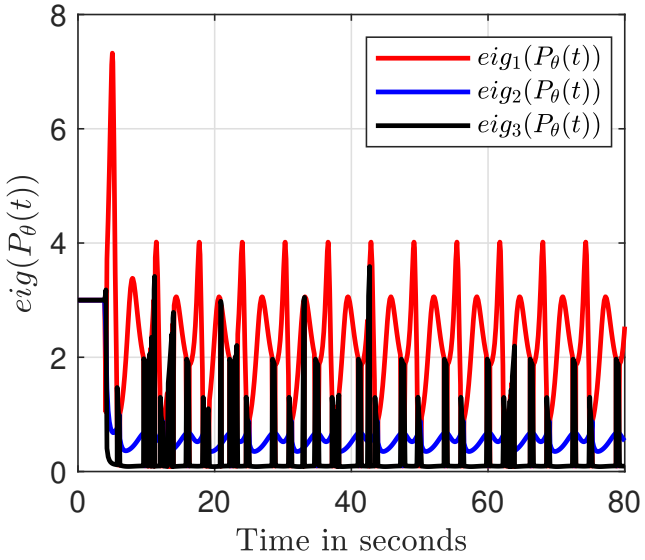


Fig. 4. Eigen values of the matrix $P_\theta(t)$ as a function of time.

that satisfies $Z_{11}(t) \prec 0$ and 2) verify that (55) is satisfied for a predefined value of $Q$. Condition (55) is satisfied for all $t \geq t_f$ for a constant value of $P_X(t)$=$P_X$=0.5 and for $Q(t)$=$0.67I_{4\times4}$ where $L(t)$ is calculated by locating the poles of $A(t) + K(t)\tilde{T}(t)$ at -2 for all $t \geq t_F$. The values corresponding to $L(t)$ are plotted on Figure 3. The placement starts after $t_F$= 4 s and $L(t)$ exhibits an oscillatory behavior due to the dynamics of $A(t)$. The adaptive observer is started from the following initial conditions: $\hat{u}_0(x) = -4$, $\hat{v}_0(x) = -4$, $\hat{X}(0) = -1$, $\hat{\theta}_1(0) = 4$, $\hat{\theta}_2(0) = 10$, $\hat{\theta}_3(0) = -13$. The convergence of the PDEs and the ODEs estimation errors are shown on Figure 5 and 6, respectively. After $t_F$=4 s, the estimation errors start converging to zero after exhibiting some oscillatory transients. The parameter estimations are shown on Figure 6. The adaptation starts after 4 seconds and the parameter estimations converge to their true values after approximately 20 seconds. Finally, the norm $V(t) = \left|\tilde{X}\right|^2 + |\tilde{\theta}|^2 + ||E(.,t)||^2_{(\mathbb{L}^2([0,1]))^2}$ of Theorem 4 is shown on Figure 7. It increases on the interval of time $[0, 4\,s]$ due to the unstable dynamics $A(t)$ and the presence of no observer gain $L(t)$=0, but it decays to zero in nearly 20 seconds after the injection of the system measurements.

## 5 Application to cooling plants

Consider the refrigeration cycle that is depicted on Figure 1. The objective is to design an estimator that uses measurements from the three temperature sensors to estimate the in-domain temperatures and the heat transfer coefficient of the heat exchanger, and the temperature of the heater. We begin by giving the mathematical equations that model the coupled exchanger-heater system.

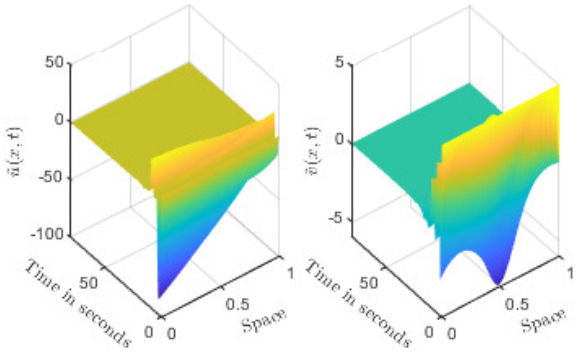


Fig. 5. Unstable plant: PDE estimation errors.

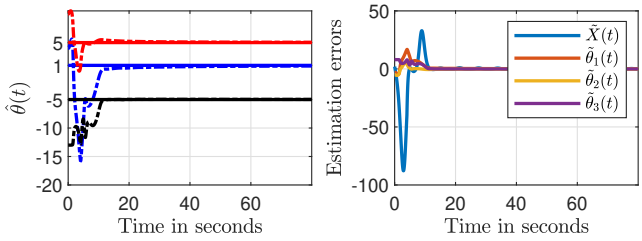


Fig. 6. Unstable plant: evolution of the estimated parameters $\theta$ (left) and of $\tilde{X}(t)$ and $\tilde{\theta}(t)$ (right).

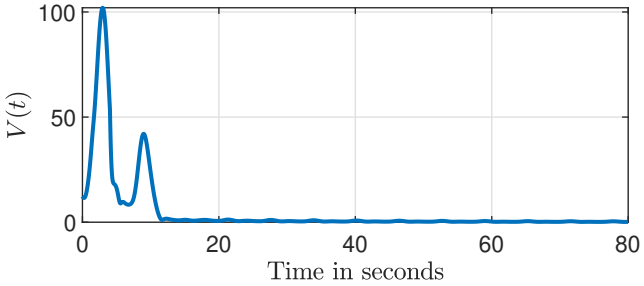


Fig. 7. Unstable plant: evolution of the Lyapunov function $V(t)$.

### 5.1 Model dynamics

We model the coupled exchanger-heater system based on the following assumptions. For the heat exchanger, we take the same assumptions taken by the authors in [15, Section 4]. For the heater, we assume that the temperature is uniform along the length and the heater is well insulated from the surroundings. Based on these assumptions, the coupled exchanger/heater system has

Table 1
Nomenclature of cooling plant parameters

| Symbol | Description | Unit |
|---|---|---|
| $\rho$ | Density of water | $Kg/m^3$ |
| $\dot{m}$ | Mass flow rate | Kg/s |
| $h$ | Heat transfer coefficient (HTC) | $W/m^2.K$ |
| $A^H$ | Outer-tube cross-section area | $m^2$ |
| $A^C$ | Inner-tube cross-section area | $m^2$ |
| $D_1$ | Inner tube diameter | m |
| $C_P$ | Specific heat of water at constant pressure | J/Kg.K |
| $V^{EH}$ | Volume of the heater | $m^3$ |
| $L$ | Length of the heat exchanger | m |

the following dynamics (see [7] and [28]):

$$\partial_t T^H(x,t) + \lambda_1 \partial_x T^H(x,t) = -k_1 h(T^H(x,t) - T^C(x,t)) \tag{61}$$

$$\partial_t T^C(x,t) - \lambda_2 \partial_x T^C(x,t) = k_2 h(T^H(x,t) - T^C(x,t)) \tag{62}$$

$$T^H(0,t) = T^{EH}(t) \tag{63}$$

$$T^C(1,t) = T^C_{in}(t) \tag{64}$$

$$\dot{T}^{EH}(t) = -a(T^{EH}(t) - T^C(0,t)) + bQ_h(t) \tag{65}$$

with the following known parameters

$$\lambda_1 = \frac{\dot{m}}{LA^H\rho} \quad k_1 = \frac{\pi D_1}{A^H \rho C_p} \quad a = \frac{\dot{m}}{\rho V^{EH}}$$
$$\lambda_2 = \frac{\dot{m}}{LA^C\rho} \quad k_2 = \frac{\pi D_1}{A^C \rho C_p} \quad b = \frac{1}{C_p \rho V^{EH}}$$

where $\dot{m}$ is the mass flow rate, $L$ is the heat exchanger length, $A^H$ is the cross-sectional area of the heat exchanger outer tube, $A^C$ is the cross-sectional area of the heat exchanger inner tube, $D_1$ is the diameter of the inner tube of the heat exchanger, $\rho$ is the density of water, $C_p$ is the specific heat of water at constant pressure, $h$ is the heat transfer coefficient and $V^{EH}$ is the volume of the heater. The SI units for all the parameters are given in Table 1. The coupled exchanger/heater system has three states: the hot water temperature along the length of the heat exchanger $T^H(x,t)$, the temperature of the cold water along the length of the heat exchanger $T^C(x,t)$ and the temperature inside the heater $T^{EH}(t)$. The evolution of the exchanger temperatures is described by the PDE dynamics (61)-(62) and the evolution of the heater temperature is described by the ODE dynamics (65). The connection between the heat exchanger and the heater is given by (63). The assumption that the temperature along the heater is uniform implies that the temperature at the hot inlet of the heat exchanger is equal to the heater temperature. $T^C_{in}(t)$ is the input cold temperature on the heat exchanger cold transfer line. It is measured by sensor 1 (see Figure 1). $U(t) = Q_h(t)$ is the heat generated by the electrical equipment. It is measured in Watts (W) and considered as known. The goal is to estimate $T^H(x,t)$, $T^C(x,t)$, $T^{EH}(t)$ and $h$ using the temperatures $T^C(1,t) = T^C_{in}(t)$, $y_2^*(t) = T^C(0,t)$ and $y_1^*(t) = T^H(1,t)$, which are measured by the temperature sensors 1, 2 and 3, respectively (see Figure 1). We use numerical simulations to evaluate the performance of the observer proposed in Section 3. The first step is to simulate the model (61)-(65) to obtain the fictitious measurements $y_1^*(t)$ and $y_2^*(t)$. Afterwards, we reformulate the dynamics of the plant (61)-(65) as the model (1)-(5) using a linearization of first order. The third step is to evaluate the effect of this linearization on the approximation of the original model. Finally, we evaluate the performance of the designed adaptive observer in predicting the states of the plant as well as the heat transfer coefficient $h$. We begin by simulating a toy example of the plant (61)-(65).

**Remark 3** *Notice that the model* (61)-(65) *is a simplified version of the model* (1)-(5). *The heater-heat exchanger system is a first step towards modeling the complete cooling cycle of Figure 1. In such scenario, knowing to handle control and estimation problems on a class of systems where PDEs are connected to LTV ODEs is of great interest. For instance, one component that is also connected to the heat exchanger is the chiller (see Figure 1). The chiller contains several components (compressor, condenser, evaporator and an expansion valve) and can be modeled as a multi-variable LTV system.*

### *5.2 Model simulation*

Consider a concentric tube heat exchanger with length $L = 1\,\text{m}$, inner tube cross-sectional area $A^C = 4.9087 \times 10^{-4}\,\text{m}^2$, outer tube cross-sectional area $A^H = 3.1416 \times 10^{-4}\,\text{m}^2$ and inner tube diameter $D_1 = 2.5\,\text{cm}$. The heater volume is $V^{EH} = 0.0982\,\text{m}^3$. The refrigerant is liquid water flowing with a mass flow rate $\dot{m} = 0.2\,\text{Kg/s}$ and has the following thermodynamical characteristics: $\rho = 1000\,\text{Kg/m}^3$ and $C_p = 4200\,\text{J/Kg.K}$. The heat transfer coefficient is $h = 3000\,\text{W/m}^2\text{.K}$. To obtain informative outputs that can be used later in the estimation algorithm, we excite the plant with two inputs. The first one is $T^C_{in}(t)$, kept constant at $T^C_{in}(t) = 10\,^\circ\text{C}$. The second input is the heating power $Q_h(t)$, modulate by several increases and decreases to excite the system frequencies as shown on Figure 8. The temperatures at time $t = 0$ are assumed uniform and are set to: $T^H_0(x) = 20\,^\circ\text{C}$, $T^C_0(x) = 10\,^\circ\text{C}$ and $T^{EH}(0) = 20\,^\circ\text{C}$. The system is discretized in Matlab2019b using the finite difference scheme with a space step $dx = 0.0204\,\text{m}$ and a time step $dt = 0.0351\,\text{s}$. We show the evolution of the plant temperatures on Figure 9. The time plots of Figure 9 show the evolution of the exchanger outputs ($y_1^*(t) = T^H(1,t)$ and $y_2^*(t) = T^C(0,t)$). The temperatures follow the input excitation $Q_h(t)$ before getting stabilized when the heating power $Q_h(t)$ is held constant after 50 minutes. Now, we proceed to the next step which is reformulating (61)-(65) as (1)-(5) by linearization.

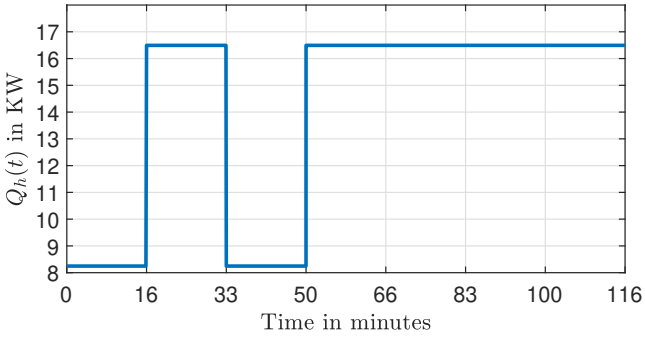


Fig. 8. Heating power $Q_h(t)$ as a function of time

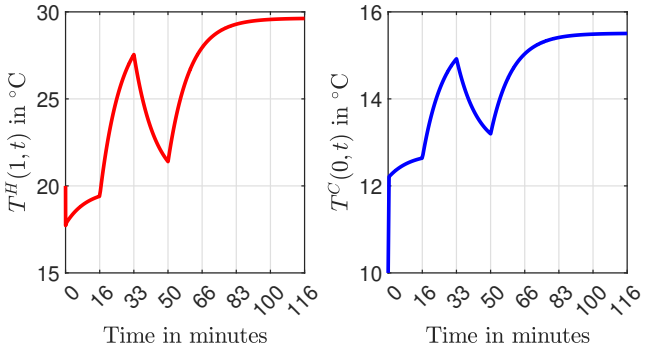


Fig. 9. Evolution of the plant output temperatures.

### *5.3 Linearization*

The main difficulty of estimating the states of (61)-(65) and the heat transfer coefficient $h$ is induced by the parametric non-linearity $h\big(T^H(x,t) - T^C(x,t)\big)$. The complexity of the problem is decreased by augmenting the vector of states of the plant (61)-(65) from $\{T^H(x,t), T^C(x,t), T^{EH}(t)\}$ to $\{T^H(x,t), T^C(x,t), T^{EH}(t), h\}$ with $\dot{h} = 0$. The idea is to calculate a nominal heat transfer coefficient $h^N$ from physical correlations (see for example [16]). The calculation is based on prior knowledge of the system operating points (for example, the range of temperatures, pressures, mass flow rates, input heating power, etc.). The model (61)-(65) is then used with $h^N$ and the nominal inputs $T^C_{in,N}$ and $Q_{h,N}$ to determine the steady state operating point $\{T^H_{N,S}(x), T^C_{N,S}(x), T^{EH}_{N,S}, h^N\}$ of the plant. We thus linearize the plant (61)-(65) around the steady state with:

$$\begin{cases} T^H(x,t) & \approx T^H_{N,S}(x) + \Delta T^H(x,t), \\ T^C(x,t) & \approx T^C_{N,S}(x) + \Delta T^C(x,t), \\ T^{EH}(t) & \approx T^{EH}_{N,S} + \Delta T^{EH}(t), \\ h & = h^N + \Delta h, \\ T^C_{in}(t) & = T^C_{in,N} + \Delta T^C_{in}(t) \\ Q_h(t) & = Q_{h,N} + \Delta Q_h(t) \end{cases} \tag{66}$$

where $\Delta$ denotes the first order variation, and we get the dynamics of the linearized system:

$$\partial_t \Delta T^H(x,t) + \lambda_1 \partial_x \Delta T^H(x,t) = -k_1 h^N \big(\Delta T^H(x,t) - \Delta T^C(x,t)\big) - k_1 \big(T^H_{N,S}(x) - T^C_{N,S}(x)\big)\Delta h \tag{67}$$

$$\partial_t \Delta T^C(x,t) - \lambda_2 \partial_x \Delta T^C(x,t) = k_2 h^N \big(\Delta T^H(x,t) - \Delta T^C(x,t)\big) + k_2 \big(T^H_{N,S}(x) - T^C_{N,S}(x)\big)\Delta h \tag{68}$$

$$\Delta T^H(0,t) = \Delta T^{EH}(t) \tag{69}$$

$$\Delta T^C(1,t) = \Delta T^C_{in}(t) \tag{70}$$

$$\Delta T^{EH}(t) = -a\big(\Delta T^{EH}(t) - \Delta T^C(0,t)\big) + b\Delta Q_h(t) \tag{71}$$

The plant model (61)-(65) is compared with the linearized model (66)-(71) as follows. The simulation of the plant model is the same as in Section 5.2 with the same parameters $h = 3000\,\mathrm{W/m^2.K}$ and with the same inputs. For the linearized model, we choose different nominal points for $h^N = \{500, 1500, 2500\}$ and we simulate (67)-(71) with the linearized inputs $\Delta T^C_{in}(t) = 0$ and $\Delta Q_h(t) = Q_h(t) - Q_{h,N}$ where $Q_h(t)$ is the heating power plotted on Figure 8 and $Q_{h,N} = 16.5\,\mathrm{KW}$ is the nominal heating input. The initial conditions for (67)-(71) are calculated from (66) and we plot on Figure 10 the relative linearization errors in (%):

$$\epsilon^H(t) = \frac{\int_0^1 |T^H(x,t) - T^H_l(x,t)|dx}{\int_0^1 T^H_{N,S}(x)dx} \times 100 \tag{72}$$

$$\epsilon^C(t) = \frac{\int_0^1 |T^C(x,t) - T^C_l(x,t)|dx}{\int_0^1 T^C_{N,S}(x)dx} \times 100 \tag{73}$$

$$\epsilon^{EH}(t) = \frac{|T^{EH}(t) - T^{EH}_l(t)|}{T^{EH}_{N,S}} \times 100 \tag{74}$$

the subscript $l$ denotes the linearized model (66)-(71). As expected, we observe that the linearization error is smaller when the nominal model is chosen close to the plant model (i.e. when $h^N$ is chosen near to $h = 3000\,\mathrm{W/m^2.K}$). The black lines corresponding to $h^N = 2500\,\mathrm{W/m^2.K}$ are below the orange and blue lines corresponding to $h^N = 1500\,\mathrm{W/m^2.K}$ and $h^N = 500\,\mathrm{W/m^2.K}$, respectively. It is also interesting to notice that the relative error in all the cases is less than 13%, suggesting that the parametric non-linearity $\big(h\big(T^H(x,t) - T^C(x,t)\big)$ is not significantly strong. The linearized model (66)-(71) is a good approximation for the plant in the ranges of interest, and we can use it to design an adaptive observer for the plant (61)-(65).

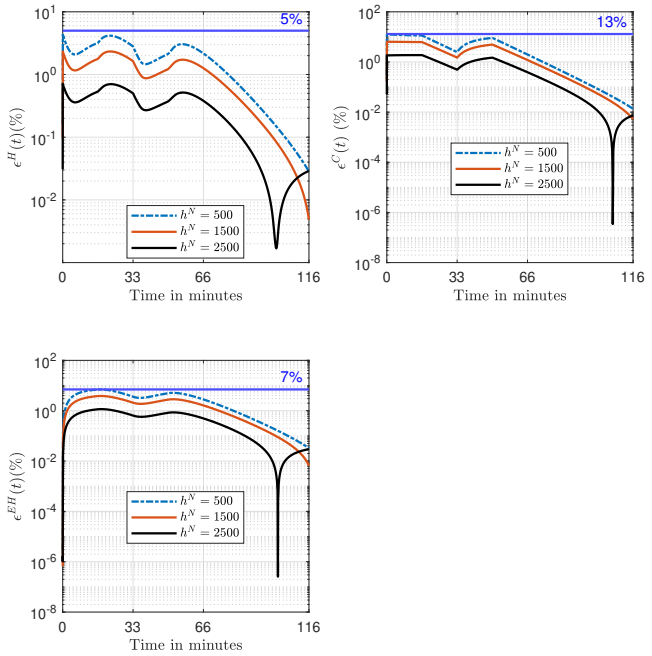


Fig. 10. Evolution of the relative linearization errors with time.

### 5.4 Observer design

We begin by reformulating (67)-(71) as (1)-(5) by defining two PDE states $u(x,t)$ and $v(x,t)$ such as

$$\Delta T^H(x,t) = e^{\frac{-k_1 h^N}{\lambda_1}x} u(x,t) \tag{75}$$

$$\Delta T^C(x,t) = e^{\frac{k_2 h^N}{\lambda_2}x} v(x,t) \tag{76}$$

$$\Delta T^{EH}(t) = X(t) \tag{77}$$

Replacing (75)-(77) in (67)-(71) one obtains

$$\partial_t u(x,t) + \lambda_1 \partial_x u(x,t) = \sigma_1(x) v(x,t) + \phi_1(x)\theta \tag{78}$$

$$\partial_t v(x,t) - \lambda_2 \partial_x v(x,t) = \sigma_2(x) u(x,t) + \phi_2(x)\theta \tag{79}$$

$$u(0,t) = X(t) \tag{80}$$

$$v(1,t) = V(t) \tag{81}$$

$$\dot{X}(t) = -aX(t) + bU(t) + av(0,t) \tag{82}$$

where $\sigma_1(x) = k_1 h^N e^{\left[\frac{k_1 h^N}{\lambda_1} + \frac{k_2 h^N}{\lambda_2}\right]x}$, $\sigma_2(x) = k_2 h^N e^{-\left[\frac{k_1 h^N}{\lambda_1} + \frac{k_2 h^N}{\lambda_2}\right]x}$, $\phi_1(x) = -k_1 e^{\frac{k_1 h^N}{\lambda_1}x}(T^H_{N,S}(x) - T^C_{N,S}(x))$ , $\phi_2(x) = -k_2 e^{\frac{-k_2 h^N}{\lambda_2}x}(T^H_{N,S}(x) - T^C_{N,S}(x))$. $\theta = \Delta h$, $V(t) = \Delta T^C_{in}(t)$ and $U(t) = \Delta Q_h(t)$. Notice that (78)-(82) is a special case of the generalized plant (1)-(5). Our plan is to design an adaptive boundary observer for (78)-(82) using the theory developed in Section 3. Once the estimates $\hat{u}(x,t)$, $\hat{v}(x,t)$, $\hat{X}(t)$ and $\hat{\theta}(t)$ are obtained, we use (75)-(77) to calculate the estimates $\Delta\hat{T}^H(x,t)$, $\Delta\hat{T}^C(x,t)$, $\Delta\hat{T}^{EH}(t)$ and $\hat{\Delta h}(t)$. Then (66) gives the temperature estimates $\hat{T}^H(x,t)$, $\hat{T}^C(x,t)$, $\hat{T}^{EH}(t)$ and an estimate for the heat transfer coefficient $\hat{h}(t)$. We start with the estimator of (78)-(82). The system (78)-(82) has the following measurements:

$$y_1(t) = e^{\frac{k_1 h^N}{\lambda_1}}\left(y_1^*(t) - T^H_{N,S}(1)\right) \tag{83}$$

$$y_2(t) = y_2^*(t) - T^C_{N,S}(0) \tag{84}$$

The over-parameterization is removed by fixing $\theta_1 = \theta_2 = \theta$ and $\theta_3 = 0$, and as a consequence the number of necessary swapping filters of the parameters drops from six to only two. The system in $T(x,t)$ remains the same but $R(x,t)$ is simplified as:

$$\begin{cases} \partial_t R_1(x,t) + \lambda_1(x)\partial_x R_1(x,t) = \sigma_1(x) R_2(x,t) \\ -p_1(x) R_1(1,t) - \phi_1(x) \\ \partial_t R_2(x,t) - \lambda_2(x)\partial_x R_2(x,t) = \sigma_2(x) R_1(x,t) \\ -p_2(x) R_1(1,t) - \phi_2(x) \\ R_1(0,t) = q R_2(0,t) \\ R_2(1,t) = 0 \end{cases} \tag{85}$$

$\hat{\theta}(t)$ is calculated using the adaptive law (29) with $\Phi(t) = [R_1(1,t), R_2(0,t)]^\top$. No change occurs on the calculation of the static observer gains $p_1(x)$ and $p_2(x)$ in (35) as well as on the calculation of $L(t)$ from condition (55). To evaluate the performance of the observer, we choose an under-estimated nominal heat transfer coefficient $h^N = 500\,\mathrm{W/m^2.K}$ and we keep the real heat transfer coefficient at $h = 3000\,\mathrm{W/m^2.K}$. We start by computing the observer gains $p_1(x)$, $p_2(x)$ and $L(t)$. The results are shown on Figure 11. The first two upper plots correspond to the static observer gains $p_1(x)$ and $p_2(x)$ with $q = 0.5$. The second left plot of Figure 11 shows the evolution of $P_\theta(t)$ in (30) as a function of time. To obtain $P_\theta(t)$, one should calculate the regressor $\Phi(t)$ by solving (85). The latter is solved in Matlab using a finite difference scheme with space step $dx = 0.0204\,\mathrm{m}$ and time step $dt = 0.0351\,\mathrm{s}$. We also fix the forgetting factor $\beta = 0.01$. We see that $P_\theta(t)$ remains bounded and positive for all $t \geq 0$. This means that the regressor $\Phi(t)$ is persistently exciting and condition (54) is satisfied. The fourth plot of Figure 11 shows the observer gain $L(t)$ as a function of time. Recall that $L(t)$ is chosen such that (55) remains satisfied for all $t \geq t_F$. We have chosen $L(t)$ such that the pole $-a + K(t)\tilde{T}(t)$ is at -0.5. Increasing or decreasing the value of this pole increases or decreases the speed of convergence of the ODE state $X(t)$. Since the ODE matrix $A(t) = A = -a$ is constant, the observer gain $L(t)$ quickly stabilizes at $L(t) = 0.496$ for $t \geq t_F$ as shown on Figure 11. Note that condition (55) is satisfied for a constant value of $P_X(t) = P_X = 1$ for all $t \geq t_F$.

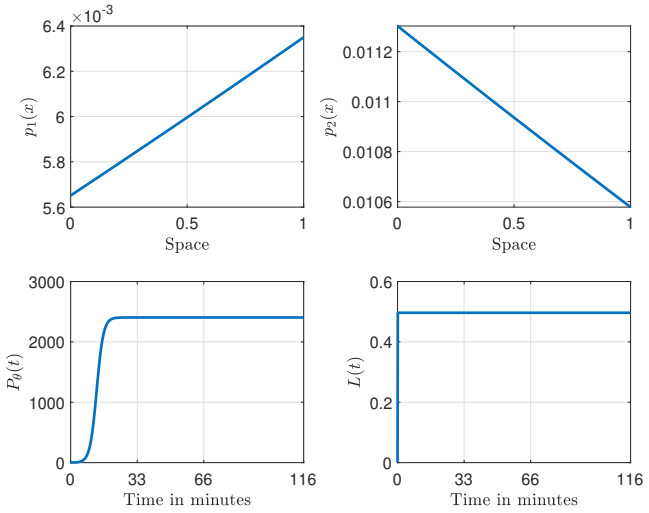


Fig. 11. Adaptive observer gains.

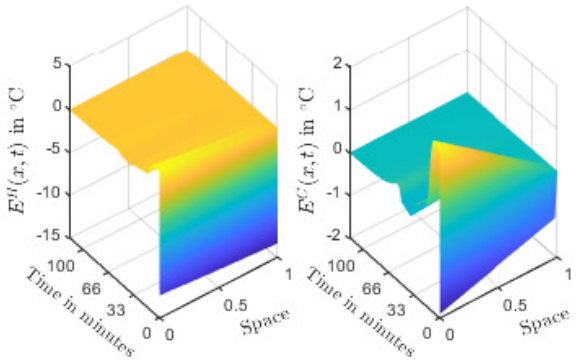


Fig. 12. $E^H(x,t) = T^H(x,t) - \hat{T}^H(x,t)$ on the left plot. $E^C(x,t) = T^C(x,t) - \hat{T}^C(x,t)$ on the right plot.

Figure 12 shows the estimation error of the temperature along the length of the exchanger. We can see that the observer succeeds in estimating the hot and the cold temperatures after a small overshoot in the beginning. The left plot of Figure 13 shows the estimation of the heater temperature. The observer estimates the temperature of the heater with high accuracy after exhibiting a small overshoot in the beginning. The right plot of Figure 11 shows the estimation of the heat transfer coefficient $h$. The estimator is initialized at the nominal value $h^N = 500\,\mathrm{W/m^2.K}$. It converges towards the real heat transfer coefficient $h = 3000\,\mathrm{W/m^2.K}$ after approximately 90 minutes. Note that the convergence of $h$ is slow. If one try to increase $\beta$, the convergence speed will not be affected. This is due to the rapid stabilization of the regressor $\Phi(t)$. Recall that $\Phi(t)$ is constructed from the steady state temperatures $(T^H_{N,S}(x), T^C_{N,S})$ in $\phi_1(x)$ and $\phi_2(x)$ using (85). The linearization of the system (61)-(65) around a dynamic trajectory $(T^H_{N,S}(x,t), T^C_{N,S}(x,t))$, as in [15, Section 4], introduces more dynamics in $\Phi(t)$ and helps in increasing the convergence rate by increasing $\beta$.

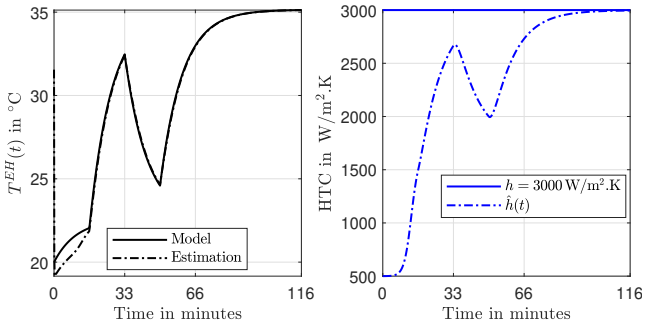


Fig. 13. Estimation of the heater temperature (left plot) and estimation of the HTC (right plot).

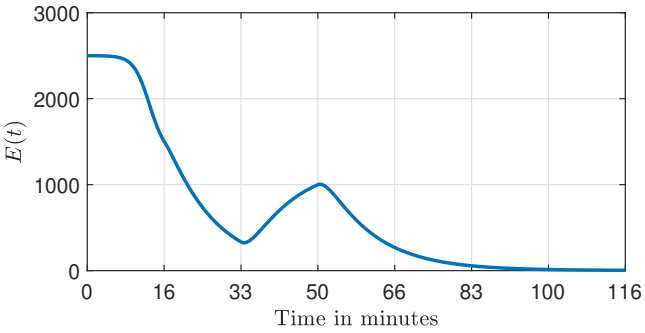


Fig. 14. E(t) as a function of time.

Figure 14 shows the evolution of the $L^2$ norm of the estimation error given by

$$E(t) = \Bigg( \int_0^1 \left|T^H(x,t) - \hat{T}^H(x,t)\right|^2 + \left|T^C(x,t) - \hat{T}^C(x,t)\right|^2 dx + \left|T^{EH}(t) - \hat{T}^{EH}(t)\right|^2 + \left|h - \hat{h}(t)\right|^2 \Bigg)^{1/2} \tag{86}$$

$E(t)$ is stabilizing at zero after exhibiting some transients due to the observer initial conditions. The observer succeeds in estimating every temperature along the length of the exchanger as well as the heater temperature and the heat transfer coefficient $h$.

## 6 Conclusion

In this paper, we have solved the problem of estimating the temperatures and the HTC of a coupled heat exchanger-heater system. The estimation problem is formulated on a more general class of systems with coupled hyperbolic PDEs and LTV ODEs. The observer design is based on swapping design theory, backstepping transformation theory, parameter estimation theory and the Lyapunov theory for stability analysis. The performance of the observer is first evaluated successfully in numerical simulations for an unstable plant. Considering the cooling plant, simulations show that the observer with

only three sensor inputs is able to estimate the temperatures inside the exchanger as well as the HTC. A directly related future topic is the experimental validation of the observer, which would allow to compare the quality of the temperature estimations of the observer with three sensors to the observer with four sensors developed by [15]. Another interesting topic is to solve the problem of estimating the HTC and the temperature states without the linearization step in Section 5.3. It is also interesting to consider the change of phase that could occur in the heat exchanger. This will introduce nonlinearites to the system along with additional dynamics to account for the multiple phases.

## References


[1] H. Anfinsen and O. M. Aamo. State estimation in hyperbolic PDEs coupled with an uncertain LTI system. In *2017 American Control Conference (ACC)*, pages 3821–3827. IEEE, 2017.

[2] H. Anfinsen and O. M. Aamo. *Adaptive Control of Hyperbolic PDEs*. Communications and Control Engineering. Springer International Publishing, 2019.

[3] H. Anfinsen, M. Diagne, O. M. Aamo, and M. Krstic. An adaptive observer design for $n+1$ coupled linear hyperbolic PDEs based on swapping. *IEEE Transactions on Automatic Control*, 61(12):3979–3990, 2016.

[4] H. T. Banks and M. A. Demetriou. Adaptive parameter estimation of hyperbolic distributed parameter systems: Non-symmetric damping and slowly time varying systems. *ESAIM: COCV*, 3:133–162, 1998.

[5] G. Bastin and J.-M. Coron. *Stability and boundary stabilization of 1-d hyperbolic systems*, volume 88. Springer, 2016.

[6] P. Bernard and M. Krstic. Adaptive output-feedback stabilization of non-local hyperbolic PDEs. *Automatica*, 50(10):2692–2699, 2014.

[7] F. Bonne. *Modélisation et contrôle des grands réfrigérateurs cryogéniques*. Theses, Université de Grenoble, Dec. 2014.

[8] F. Castillo, E. Witrant, C. Prieur, and L. Dugard. Boundary observers for linear and quasi-linear hyperbolic systems with application to flow control. *Automatica*, 49(11):3180–3188, 2013.

[9] R. Curtain, M. Demetriou, and K. Ito. Adaptive observers for structurally perturbed infinite dimensional systems. In *Proceedings of the 36th IEEE Conference on Decision and Control*, volume 1, pages 509–514, 1997.

[10] J. Deutscher, N. Gehring, and R. Kern. Output feedback control of general linear heterodirectional hyperbolic ODE–PDE–ODE systems. *Automatica*, 95:472–480, 2018.

[11] F. Di Meglio, P.-O. Lamare, and U. J. F. Aarsnes. Robust output feedback stabilization of an ODE–PDE–ODE interconnection. *Automatica*, 119:109059, 2020.

[12] I. Dincer. *Refrigeration systems and applications*. John Wiley & Sons, 2017.

[13] F. Ferrante and A. Cristofaro. Boundary observer design for coupled ODEs–hyperbolic PDEs systems. In *2019 18th European Control Conference (ECC)*, pages 2418–2423, 2019.

[14] M. Ghousein and E. Witrant. Adaptive boundary observer design for coupled ODEs-hyperbolic PDEs systems. *IFAC-PapersOnLine*, 53(2):7605–7610, 2020.

[15] M. Ghousein, E. Witrant, V. Bhanot, and P. Petagna. Adaptive boundary observer design for linear hyperbolic systems; application to estimation in heat exchangers. *Automatica*, 114:108824, 2020.

[16] V. Gnielinski. New equations for heat and mass transfer in turbulent pipe and channel flow. *Int. Chem. Eng.*, 16(2):359–368, 1976.

[17] A. Hasan, O. M. Aamo, and M. Krstic. Boundary observer design for hyperbolic PDE–ODE cascade systems. *Automatica*, 68:75–86, 2016.

[18] L. Hu, F. Di Meglio, R. Vazquez, and M. Krstic. Control of homodirectional and general heterodirectional linear coupled hyperbolic PDEs. *IEEE Transactions on Automatic Control*, 61(11):3301–3314, 2016.

[19] P. A. Ioannou and J. Sun. *Robust adaptive control*, volume 1. PTR Prentice-Hall Upper Saddle River, NJ, 1996.

[20] M. Krstic and A. Smyshlyaev. Backstepping boundary control for first-order hyperbolic PDEs and application to systems with actuator and sensor delays. *Systems & Control Letters*, 57(9):750–758, 2008.

[21] F. D. Meglio, D. Bresch-Pietri, and U. J. F. Aarsnes. An adaptive observer for hyperbolic systems with application to underbalanced drilling. *IFAC Proceedings Volumes*, 47(3):11391–11397, 2014. 19th IFAC World Congress.

[22] W. Rugh. *Linear system theory*, volume 2. prentice hall Upper Saddle River, NJ, 1996.

[23] R. Vazquez, M. Krstic, and J.-M. Coron. Backstepping boundary stabilization and state estimation of a $2\times$ 2 linear hyperbolic system. In *Decision and Control and European Control Conference (CDC-ECC), 2011 50th IEEE Conference on*, pages 4937–4942. IEEE, 2011.

[24] B. Verlaat, M. Van Beuzekom, and A. Van Lysebetten. CO2 cooling for HEP experiments. In *Topical Workshop on Electronics for Particle Physics (TWEPP-2008), Naxos, Greece*, pages 328–336, 2008.

[25] S. A. Wadoo. Adaptive control of a hyperbolic partial differential equation system with uncertain parameters. In *15th International IEEE Conference on Intelligent Transportation Systems*, pages 608–612, 2012.

[26] E. Witrant and S.-I. Niculescu. Modeling and control of large convective flows with time-delays. *Mathematics in Engineering, Science and Aerospace*, 1(2):191–205, 2010.

[27] C.-Z. Xu and G. Sallet. Exponential stability and transfer functions of processes governed by symmetric hyperbolic systems. *ESAIM: Control, Optimisation and Calculus of Variations*, 7:421–442, 2002.

[28] Z. Xu, R. Diao, S. Lu, J. Lian, and Y. Zhang. Modeling of electric water heaters for demand response: A baseline pde model. *IEEE Transactions on Smart Grid*, 5(5):2203–2210, 2014.

[29] H. Yu and M. Krstic. Traffic congestion control for aw–rascle–zhang model. *Automatica*, 100:38–51, 2019.

[30] Y. Zhu, M. Krstic, and H. Su. Adaptive output feedback control for uncertain linear time-delay systems. *IEEE Transactions on Automatic Control*, 62(2):545–560, 2017.

[31] F. Zobiri, E. Witrant, and F. Bonne. PDE observer design for counter-current heat flows in a heat-exchanger. *IFAC-PapersOnLine*, 50(1):7127–7132, 2017.